8-23
5-29-77

HB. 1448

LA-6930-MS
Informal Report

UC-66a

Issued: August 1977

Petrography and Geochemistry of Precambrian Rocks from GT-2 and EE-1

A. William Laughlin
Andrea Eddy

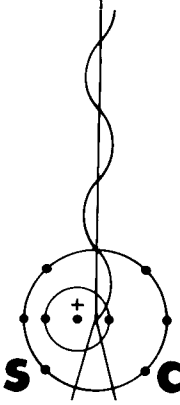

los alamos
scientific laboratory
of the University of California
LOS ALAMOS, NEW MEXICO 87545

UNITED STATES
ENERGY RESEARCH AND DEVELOPMENT ADMINISTRATION
CONTRACT W-7405-ENG. 36

DISCLAIMER

PETROGRAPHY AND GEOCHEMISTRY OF PRECAMBRIAN ROCKS FROM GT-2 AND EE-1

by

A. William Laughlin and Andrea Eddy

ABSTRACT

During the drilling of GT-2 and EE-1, 27 cores totaling about 35 m were collected from the Precambrian section. Samples of each different lithology in each core were taken for petrographic and whole-rock major- and trace-element analyses. Whole-rock analyses are now completed on 37 samples. From these data we recognize four major Precambrian units at the Fenton Hill site. Geophysical logs and cuttings have been used to extrapolate between cores. The most abundant rock type is an extremely variable gneissic unit comprising about 75% of the rock penetrated. This rock is strongly foliated and may range compositionally from syenogranitic to tonalitic over a few centimeters. The bulk of the unit falls within the monzogranite field. Interlayered with the gneiss is a ferrohastingsite-biotite schist which compositionally resembles a basaltic andesite. A fault contact between the schist and gneiss was observed in one core. Intrusive into this metamorphic complex are two igneous rocks. A leucocratic monzogranite occurs as at least two 15-m-thick dikes, and a biotite-granodiorite body was intercepted by 338 m of drill hole. Both rocks are unfoliated and equigranular. The biotite granodiorite is very homogeneous and is characterized by high modal contents of biotite and sphene and by high K_2O, TiO_2, and P_2O_5 contents. Although all of the cores examined show fractures, most of these are tightly sealed or healed. Calcite is the most abundant fracture filling mineral, but epidote, quartz, chlorite, clays or sulfides have also been observed. The degree of alteration of the essential minerals normally increases as these fractures are approached. The homogeneity of the biotite granodiorite at the bottom of GT-2 and the high degree of fracture filling ensure an ideal setting for the Hot Dry Rock Experiment.

I. INTRODUCTION

The Los Alamos Scientific Laboratory (LASL) of the University of California has recently drilled two deep boreholes in the Jemez Mountains of north-central New Mexico. The 2.93-km Geothermal Test Hole No. 2 (GT-2), completed in December 1974, penetrated 0.73 km of Paleozoic and Cenozoic rocks and 2.20 km into the Precambrian basement. The other hole, Energy-Extraction Hole No. 1 (EE-1), is the first of two to be used to demonstrate a technique for extracting geothermal energy from hot, low permeability rock (Smith[1]). EE-1 is 77 m (253 ft) N14°E of GT-2. The drilling of EE-1 was temporarily halted in October 1975 at a depth of 3.06 km.

Of the 27 cores recovered, most are from GT-2; 25 are from Precambrian rocks. In addition, cuttings were collected at about 1.5-m intervals during the entire drilling of GT-2, and at 3-m intervals in EE-1. Several complete suites of geophysical logs were run in both holes (West et al.[2]).

Because of the great depth of Precambrian rocks penetrated, the high equilibrium bottom-hole temperatures (197°C in GT-2, 205°C in EE-1), and the availability of supporting geophysical data, a large number of chemical and isotopic studies of the core samples are in progress. In this report, we present the results of initial petrographic and major-element whole-rock chemical analyses of the Precambrian rocks. The results of trace-element, geochronological, and stable-isotopic studies will be reported later.

II. LOCATION AND GEOLOGIC SETTING OF GT-2 AND EE-1

The drilling site for GT-2 and EE-1 is located on Fenton Hill in the NE 1/4, Sec 13, T19N, R2E, Sandoval County, New Mexico. The site is 32 km west of Los Alamos within the Santa Fe National Forest with access provided by New Mexico Highway 126. (Fig. 1).

The Fenton Hill site is on the western flank of the Valles Caldera at an elevation of 2469 m (8690 ft). Because the geology of the caldera and its environs has been extensively discussed in the literature, only a brief summary will be given here. The interested reader can refer to the work of Smith et al.,[3,4] Smith and Bailey,[5] Ross et al.,[6] Bailey et al.,[7] and Doell et al.,[8] for additional information on this area. Several reports by LASL personnel (Purtymun,[9] West,[10] and Purtymun et al.[11]) have related the local geology to our geothermal project.

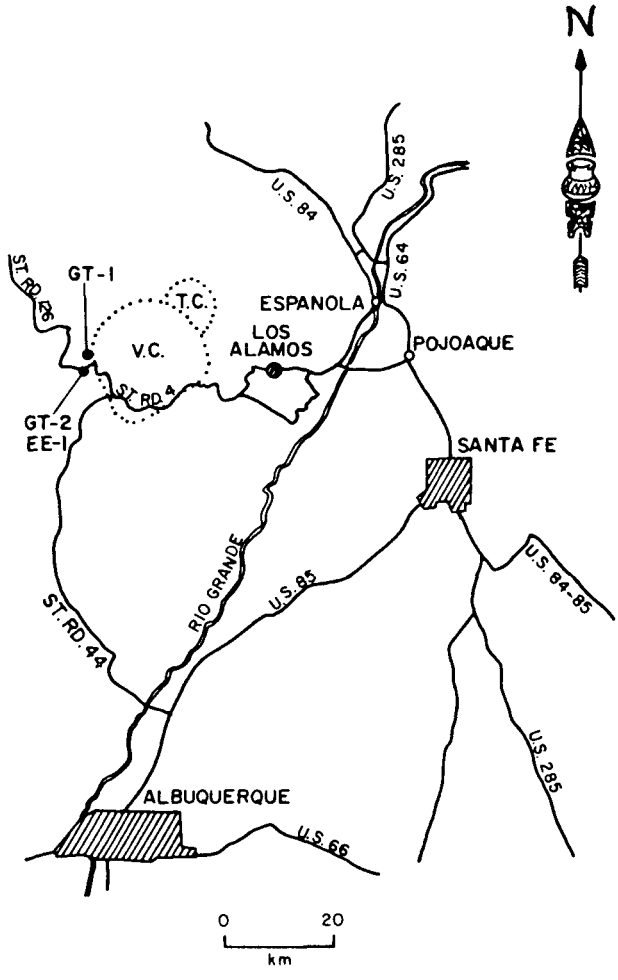

Fig. 1. Locations of geothermal test holes GT-1 and GT-2. (Dotted lines indicate approximate geologic boundaries of the Valles Caldera, V.C., and the Toledo Caldera, T.C.).

Surface rocks at the drilling site are part of the Bandelier Tuff, which is of late-Cenozoic age (1.1- to 1.4-Myr old, Doell et al.[8]). This tuff was ejected from the Valles and Toledo Calderas causing the development of a 19- to 24-km-diam (12- to 15-mile) collapse feature. Later activity produced a central resurgent (structural) dome and a ring of extrusive rhyolite domes within the Valles Caldera. The final activity was associated with the El Cajete Crater on the southwest flank of the resurgent dome. It produced the Battleship Rock, El Cajete,and Banco Bonito Members of the Valles Rhyolite. The El Cajete Member is older than 0.042 Myr and younger than 0.1 Myr. Thermal springs are still common in the area.

Data on the rocks underlying the Bandelier Tuff are summarized in Table I. The Phanerozoic Section is based on five boreholes drilled prior to GT-2 and EE-1, four shallow ones drilled for heat-flow measurements and a deeper test hole (GT-1) which penetrated the Precambrian basement. In brief, beneath the Bandelier Tuff in descending order, are the Cenozoic Paliza Canyon and Tschicoma Formations and the Abiquiu Tuff, the Permian Abo Formation, the Pennsylvanian Magdalena Group, and Precambrian crystalline rocks. Individual units vary greatly in thickness between boreholes and in some holes they may be absent altogether.

LASL's first deep borehole (GT-1) penetrated 143 m (469 ft) of Precambrian rocks. Perkins[12] studied samples of these rocks and compared them to Precambrian rocks exposed in the area. The latter included samples from the nearest Precambrian outcrops, at Soda Dam and in Guadalupe Box, as well as from the Nacimiento, San Pedro, and Sandia Mountains. Soda Dam is on the Jemez River about 9 km south of the GT-2 site and Guadalupe Box is another 16 km to the south-southwest.

DuChene[13] has discussed the structural geology of the Guadalupe Box area and Woodward et al.[14] have summarized the available petrologic data on the Precambrian rocks of the southern Nacimiento Mountains, which lie west of our drill site. According to Woodward et al.,[14] quartz-monzonitic (or monzogranitic, approximate IUGS equivalent: see Section V.B.) to granodioritic gneisses are the most abundant metamorphic rocks within the southern Nacimientos. These rocks may be either leucocratic or biotite-rich. Minor amounts of amphibolite, hornblendite, muscovite-quartz schist, and mafic xenoliths are also present. In the central portion of the area, the Joaquin granite has widespread exposures. Woodward et al.[14] concluded from textural evidence that this rock had an igneous origin.

Although the structural geology of the Fenton Hill area is fairly simple, several faults are present. The closest of these is the locally north-south-trending caldera ring fault about 3 km east of the site. This fault is downthrown 91 to 122 m (200 to 400 ft) to the east.[11] About 4 km southeast of the site is the northeast-trending Virgin Canyon fault, downthrown to the southeast. Also trending northeast is the Jemez fault, 6 km southeast of the site.[11] The Jemez fault is downthrown to the southeast; its throw varies from 244 to 305 m (800 to 100 ft).[11]

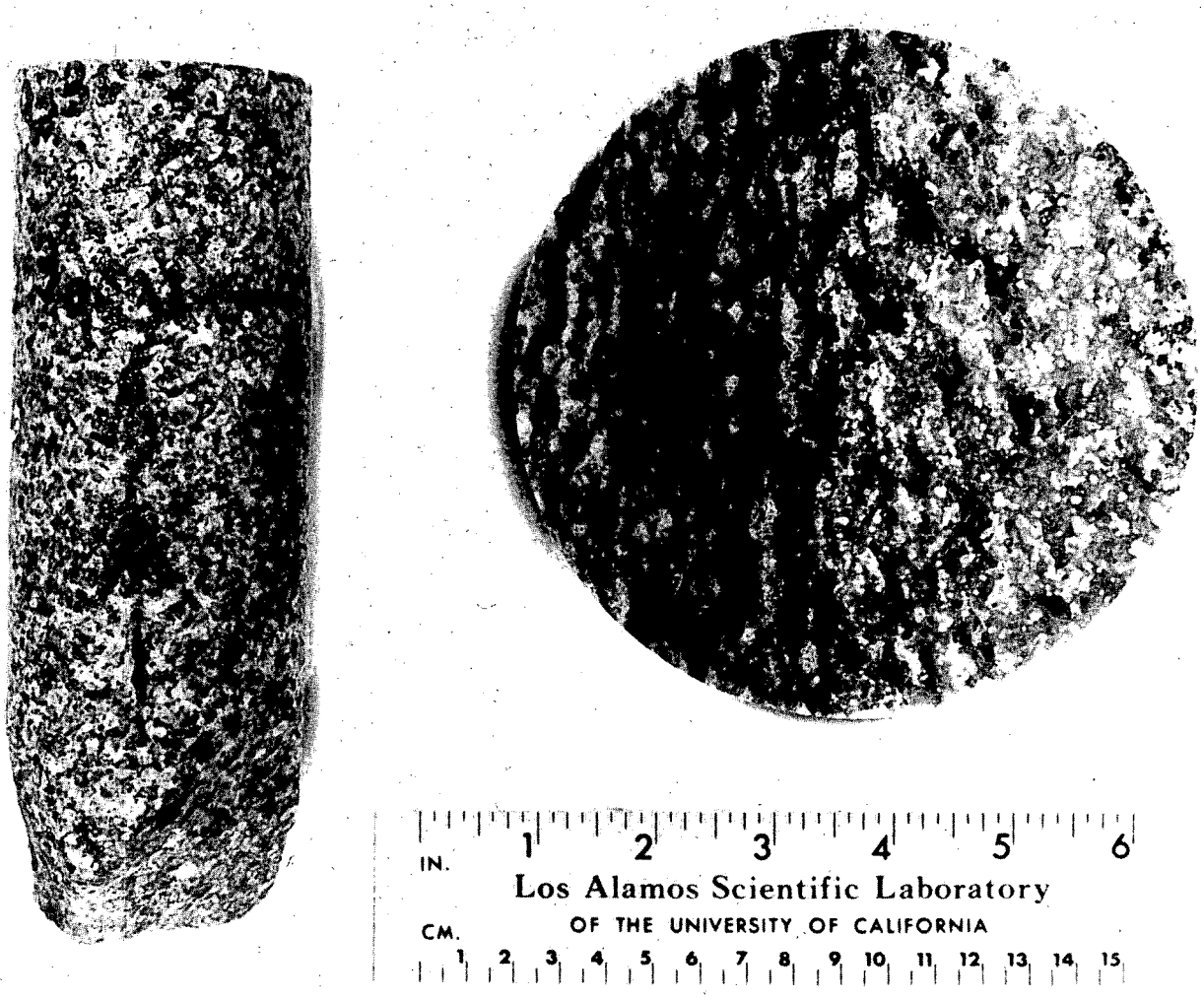

Fig. 2. Left: JOIDES core (62-mm-diam) from 2905-m (9531-ft) depth, of biotite granodiorite.
Right: Christiansen diamond core (133-mm-diam) from 2165-m (7102-ft) depth, of biotite-tonalite gneiss (darker portion) and leucocratic monzogranite gneiss.

III. CORING HISTORY OF GT-2

Two different methods of coring were employed during the drilling of GT-2 and EE-1. A modified JOIDES core bit was used to produce an unoriented 62-mm-diam (2.44-in.) core (Fig. 2, left). A few cores were obtained using a conventional 133-mm-diam (5.25-in.) diamond core bit designed to produce an oriented core (Fig. 2, right). However, some of the cores recovered using this second method were unoriented because of rotation in the core barrel or film failure in the orienting device due to the high temperatures at depth.

Twenty-five cores were obtained from GT-2 (Table II). Five of these were the larger diamond cores and the rest were obtained with the JOIDES bits. Recoveries varied from less than 10% to 100%; the diamond coring yielded total return. The total recovered core length was about 35 m. Although two cores were recovered from the Paleozoic section, only the Precambrian cores will be discussed in this report.

IV. METHODS OF STUDY

The cores were washed with distilled water at the drill site where a preliminary log sheet was prepared. The core was then packaged in transparent plastic tubes for transport to our laboratory. All cores were photographed in color, the core being rotated 120 degrees between exposures to ensure complete surface coverage. At this time the individual pieces of core were numbered and a more complete log prepared. This record included megascopic identification of lithologies, number and orientation of fractures where possible, and types of fracture fillings.

Each lithology within each core was sampled, a thin section prepared, and splits taken for whole-rock and trace-element chemistry. Splits were also taken for rubidium-strontium isotopic studies. Mineral separation is now under way to prepare samples for potassium-argon, fission-track, and uranium-thorium-lead geochronological studies. Selected samples have also been taken for stable-isotope and fluid-inclusion geothermometry.

Standard petrographic methods were used in the core studies. Mineral determinations from thin sections were based on physical characteristics such as color, form, cleavage, relief, twinning, association and alteration, and optical properties including birefringence, angle of extinction, pleochroism and absorption, optic sign, optic axial angle and crystallographic orientation. Plagioclase feldspar compositions were determined by extinction angles in sections normal to (010) (Clarke and Eddy[15]) and optic sign. A standard polarizing microscope and manual point counter were used in the modal analyses. The statistics applied to the major minerals (Table III) are based on Van der Plas and Tobi.[16] It should be noted, however, that the distance between points was usually smaller than the largest grain size in a given section, thus making the 2σ values less dependable. The point-grid size was chosen to yield over 1000 points per sample where possible. Mineral grain-size categories used in

petrographic descriptions are: fine-grained, <1-mm diam; medium-grained, 1- to 5-mm diam; and coarse-grained, >5-mm diam.

Using a combination of analytical techniques, chemical analyses (Table V) were performed by John Husler, University of New Mexico (UNM). Atomic absorption spectrophotometry was used to determine aluminum, total iron, magnesium, calcium, sodium, potassium, titanium, manganese, and strontium. Silicon was determined gravimetrically and phosphorus colorimetrically using the phosphomolybdate method. Ferrous iron was determined volumetrically by titration with potassium dichromate. Water (H_2O^-) was determined by weight loss at 110°C and H_2O^+ by loss on ignition at 1000°C after compensation for oxidation of ferrous to ferric iron. The precision for silicon is ±1% of the amount present and for the other oxides is ±2% of the amount present. Accuracy was monitored by the use of USGS standard rock samples.

In this report sample numbers, unless prefaced by EE-1, refer to samples from GT-2 cores.

V. RESULTS

A. Megascopic Aspects of the Cores

Two notable features are immediately apparent when the cores are examined. First is a marked diversity of texture and, to a lesser extent, of composition, both within and among individual cores. Second, there are large differences in the number of fractures and degree of rock alteration; these are most apparent between individual cores.

On the basis of texture and mineralogy, the Precambrian rocks can be roughly classified as gneissic, schistose, granitoid, or pegmatoid.

The granitoid rocks are medium- to coarse-grained light-gray or pink rocks composed primarily of quartz, plagioclase, and microcline with lesser and varying amounts of biotite and chlorite. These rocks are present in two intervals of the holes. Cuttings and spectral gamma logging were used to determine the extent of these intervals. The first of these intervals extended from 1295.4 m to 1310.6 m in GT-2 (1305.4 m to 1317.6 m in EE-1) and consisted of medium-grained pink monzogranite. The second interval, made up of light-gray biotite granodiorite, extended from 2590.8 m to near the bottom of the hole in GT-2 (Fig. 2, left).

Minor pegmatoid bodies occur throughout the hole. These are uniformly simple in composition, consisting mainly of quartz, microcline, and minor

plagioclase and micas. Although structural relationships are difficult to determine because of core size, these pegmatites usually appear to be tabular bodies discordant to the gneissic foliation.

Gneissic rocks make up the bulk of the Precambrian rocks encountered (Fig. 2, right). They are usually somewhat darker in color than the granitoid rocks because of higher biotite and chlorite contents. Also microcline in the gneissic rocks is usually a darker pink color than that in the granitoid rocks.

Interlayered with the gneissic rocks are many intervals of biotite schist grading into amphibolite, as in two GT-2 cores, Nos. 15 and 16 (see Table II). The cuttings and spectral gamma log indicate that such rocks are common in the hole. From the spectral gamma log we estimate that about eight percent of the Precambrian section is biotite schist.

Because stress from the coring operation may create new fractures, it is difficult to determine the frequency of original fractures. Therefore we counted only visible but closed, or open and mineralized fractures. Most of the cores show a frequency of about one fracture per 8 cm. This increases in some intervals to one per cm. There are horizontal, vertical, and roughly 60-degree-dipping fractures.

Although a wide variety of minerals occur as fracture fillings, calcite is by far the most important. Less significant are epidote, hematite, quartz, clays, and sulfides. One very prominent N60°E-striking vertical fracture in GT-2 Core No. 14 contains an assemblage of quartz, clay, muscovite, biotite, calcite, and tourmaline. A complex interval of magnetite folia is cut by a set of vertical orthogonal fractures filled with pyrite and chalcopyrite. Hornblende-biotite schists in GT-2 Core No. 16 are cut by an intricate series of fractures filled with quartz, calcite, and biotite.

B. Petrography

The results of modal analysis of thin sections are presented in Table III; averaged modes are given in Table IV. In Fig. 3 we have plotted the analyses of the felsic and intermediate rocks on the quartz-alkali feldspar-plagioclase (Q-A-P) diagram recommended by the International Union of Geological Sciences (IUGS), whose system of classification we have adopted for this report.

All of the gneissic and granitoid rocks fall within Fields 3, 4, and 5 (granite, granodiorite, and tonalite) of the IUGS diagram. We have subdivided the granites into syenogranites and monzogranites and have applied adjectival

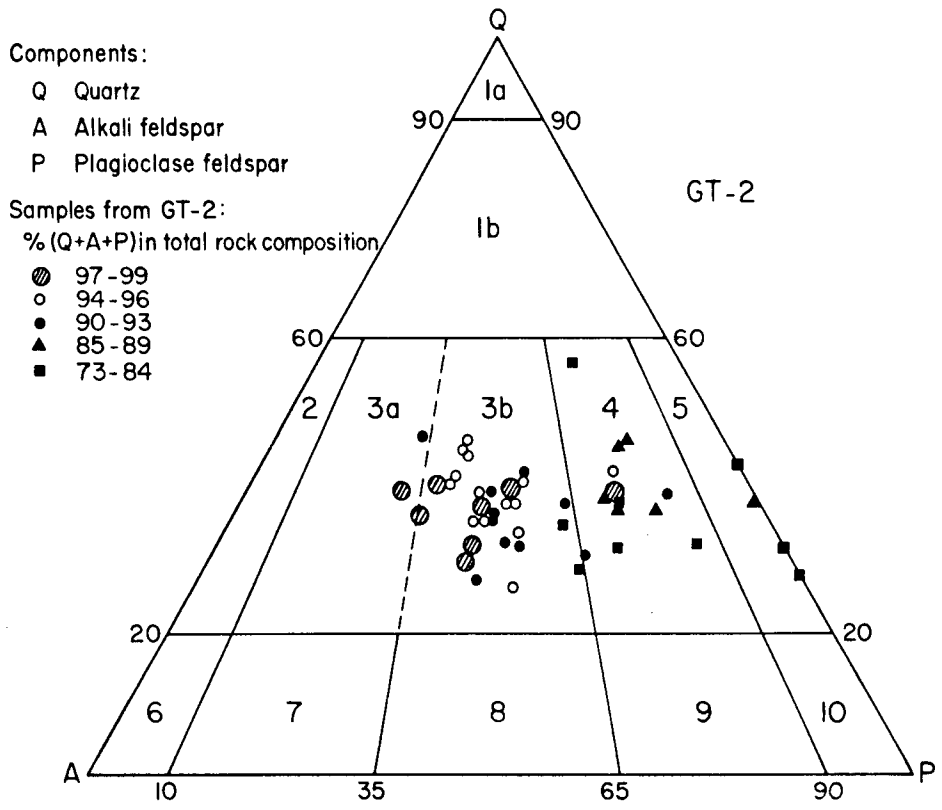

Fig. 3. Q-A-P diagram for the felsic and intermediate rocks of GT-2 (IUGS classification).

Key:
- 1a - Quartzolite (silexite)
- 1b - Quartz-rich granitoids
- 2 - Alkali-feldspar granite
- 3a - Syenogranite
- 3b - Monzogranite
- 4 - Granodiorite
- 5 - Tonalite
- 6 - Alkali-feldspar syenite
- 7 - Syenite
- 8 - Monzonite
- 9 - Monzodiorite and monzogabbro
- 10 - Anorthosite, gabbro, and diorite

modifiers where necessary to clarify the rock name. Gneissic, schistose, and granitoid rocks will be discussed separately below as textural groups.

1. Gneissic Rocks. Out of 25 Precambrian cores recovered, 21 consist of banded gneisses or schistose rocks. These metamorphic rocks make up the bulk of the Precambrian section. The gneisses are characterized by steeply dipping foliation and alternately mafic and felsic banding (Fig. 2, right). Subparallel biotite and chlorite laths are the predominant microscopic planar feature in the gneissic rocks. Sometimes elongate pods of felsic minerals, especially quartz, emphasize the gneissic structure.

Quartz, potassium feldspar, plagioclase and biotite are the dominant minerals in the gneissic rocks. These rocks range in composition from syenogranitic to tonalitic, according to the relative proportions of alkali versus plagioclase feldspar and the abundance of quartz. The mafic bands are usually granodioritic or tonalitic in composition and average 15% total mafic minerals, whereas the felsic bands, most often of granitic composition, average only 4% mafics. Less abundant minerals are alteration products such as chlorite, calcite and sericite. Myrmekite, epidote, apatite, sphene, zircon, allanite, amphibole, rutile,and opaques occur as trace or accessory minerals.

The quartz in the banded gneiss is usually strained, although it shows little or no strain in the tonalitic bands. Anhedral and clear, the quartz grains in the gneisses are usually clustered with irregular, sutured,or granulated contacts. In some samples quartz grains meet in triple points, suggestive of recrystallization. The quartz often contains fluid inclusions. The largest optically continuous quartz measured is 5.6 by 4.5 mm (in 6344-6350-3, a monzogranitic gneiss). Occasionally the quartz is considerably fractured (e.g.,in 3151-5A, a biotite-granodiorite gneiss).

The potassium feldspar in all samples is anhedral to subhedral microcline with strong grid twinning. Usually very fresh, the microcline often contains patch perthite or perthitic blebs or stringers. In some samples there are microcline megacrysts, the largest measuring 9.0 by 5.6 mm in a monzogranitic gneiss (5240-1B). Potassium-feldspar megacrysts of up to 5.6 by 2.3 mm in size are found in a biotite-granodiorite gneiss (5234-11a, 11b). At the same level, in a formerly granodioritic gneiss (5234-5), there are plagioclase grains with centers of potassium feldspar. These may have been produced by differential exsolution from plagioclase formed over a wide temperature range, or possibly by potassium released through chloritization of biotite. Also at the same

depth (5234-10) the biotite-tonalite gneiss contains antiperthite, as patchy alkali feldspar in the plagioclase.

The plagioclase in the banded gneiss ranges from An_{23} to An_{35}. It is mostly subhedral to anhedral; in the tonalitic gneisses some of the plagioclase is euhedral. Usually altered, the plagioclase is well twinned and may be slightly zoned. The plagioclase exhibits normal polysynthetic and/or rarer Carlsbad twinning. Sometimes two sets of albite twins appear to be superimposed at acute or right angles suggesting potassium feldspar, but were confirmed to be plagioclase by associated sericitization.

Often the plagioclase exhibits bent lattices or kink banding (e.g.,in 6152-3, a granite gneiss, Fig. 4a) developed in response to stress. Rarely whole plagioclase grains are considerably granulated (e.g.,in 3699-2.1, a monzogranitic gneiss). In some granite gneisses, small plagioclase grains surround larger potassium feldspars. More often granulation and sutured edges characterize the contact relations between the felsic minerals.

In rare samples (e.g.,5980-1, a granite gneiss, and 4893-1a, a biotite-tonalite gneiss) the plagioclase is quite fresh, but it is usually considerably altered, characteristically to sericite (Fig. 5). The mica most often forms at an angle to (010) of the plagioclase. Rare plagioclase alteration products are saussurite or epidote (e.g.,in 5240-1A, a biotite-granodiorite gneiss), calcite or clays. Minor zoning is emphasized by alteration confined to the cores, although in some cases there is preferential alteration of the rims. Occasionally only alternate twin sets are affected (e.g.,in 2600-3, a monzogranitic gneiss, and 2844-2, a syenogranitic gneiss). In one granodioritic (3151-1A) and one tonalitic gneiss (5234-10) alteration seems to have proceeded from the grain boundaries inwards without being zonally confined. Plagioclase alteration tends to be greater near cross-cutting fractures (Fig. 5b).

In one granodioritic gneiss (5234-5) there are alkali-feldspar-centered plagioclase grains, possibly formed by mobilized potassium or exsolution (see discussion above). Antiperthite is not uncommon as patches or blebs, whose crystallographic axes are apparently at a small angle to those of the host plagioclase. Perthite, as patches or beads of plagioclase in the alkali feldspar, is found particularly in the more felsic gneisses. Rarely the plagioclase has irregular feldspar overgrowths (e.g.,6152-3, a granite gneiss).

In several samples there is symplectic or vermicular intergrowth of plagioclase and biotite or chloritized biotite (e.g.,4892-1b1 and 5234-10, tonalitic

Fig. 4. Deformation features in GT-2 cores.

a. Above: Plagioclase showing bent crystal lattice (note deformation bands perpendicular to twinning), cross-cut by calcite-filled fracture; in leucocratic granite gneiss from the 1875-m (6152-ft) depth; crossed nicols. (Bar equals 1 mm).

b. Right, top: Deformed biotite in quartz-rich biotite-granodiorite gneiss, from the 1824-m (5985-ft) depth; plane light. (Bar equals 1 mm).

c. Right, bottom: Biotite showing kink banding, in biotite granodiorite from the 2904-m (9527-ft) depth; plane light. (Bar equals 1 mm).

gneisses). The plagioclase also often contains numerous inclusions of accessory minerals, especially in the granite gneisses.

In the gneisses of granitic composition, myrmekite averages 1%, with a maximum of 4% (in 3694-1.1); it averages less than 0.5% down to trace amounts in the more mafic gneisses. The myrmekite is anhedral and interstitial to other felsic minerals, usually plagioclase and potassium feldspar.

The biotite and chlorite occur as euhedral to subhedral laths (normal to (001)) or plates (parallel to (001)) or occasionally in anhedral interstitial

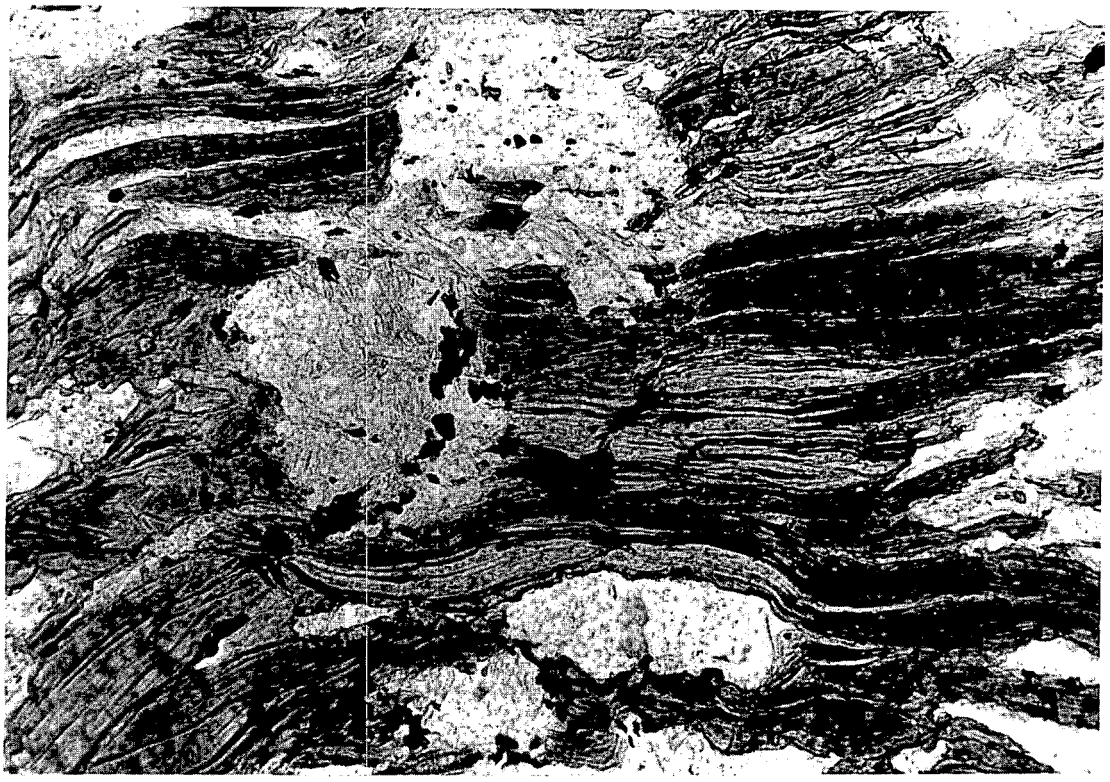

b

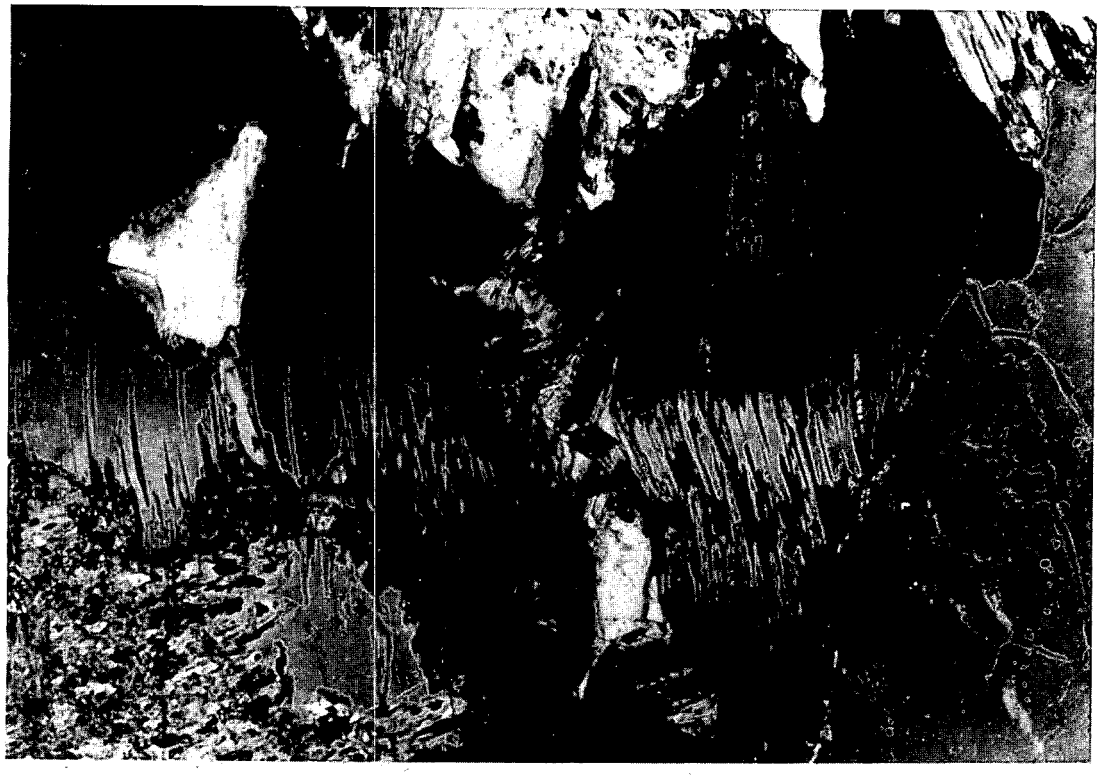

c

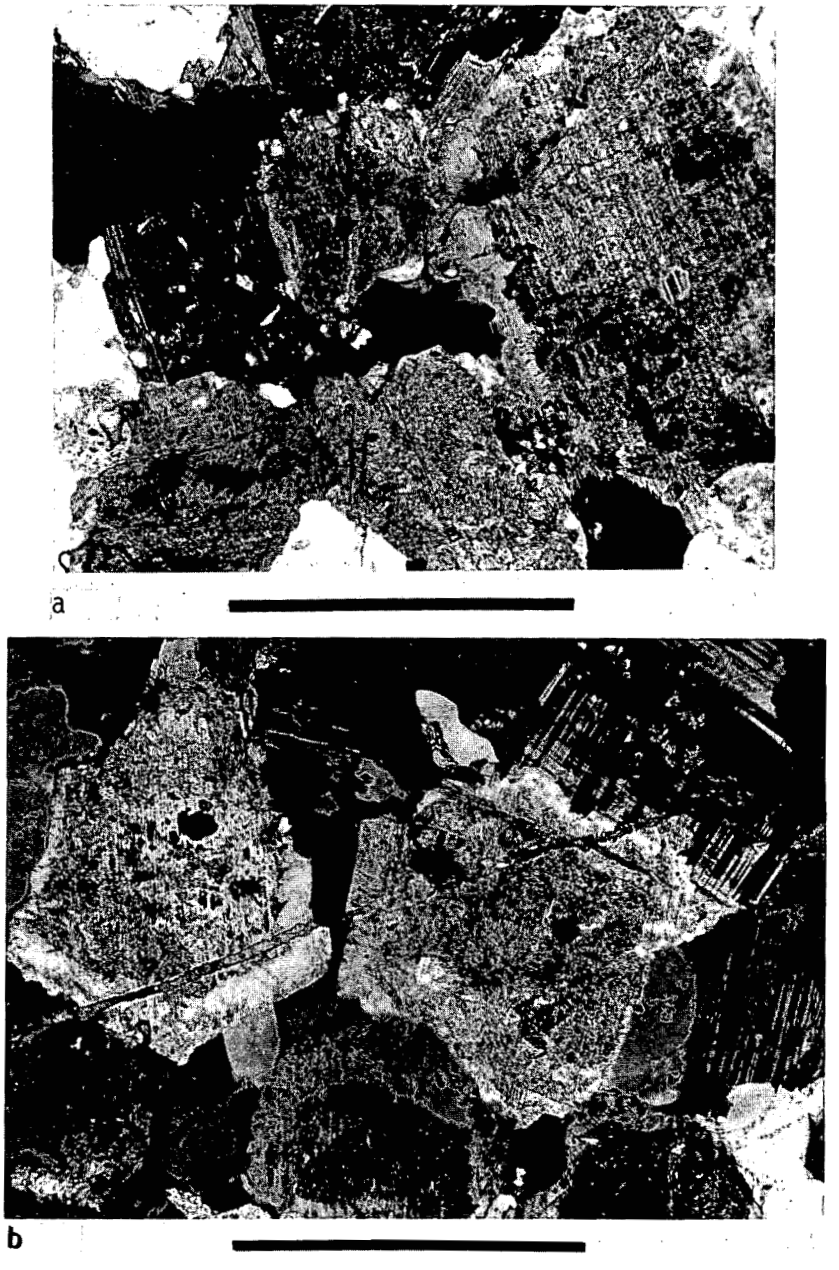

Fig. 5. Altered plagioclase in GT-2 Cores.

a. Top: Sericitized plagioclase in leucocratic granite gneiss from the 1875-m (6152-ft) depth; crossed nicols. (Bar equals 1 mm).

b. Bottom: Altered plagioclase with preferentially sericitized cores, cross-cut by calcite-filled fracture (note slight left-lateral adjustment along fracture); in granite gneiss from the 1875-m (6152-ft) depth; polarized light. (Bar equals 1 mm).

form. Commonly bands rich in subparallel biotite and chlorite laths are segregated from felsic bands in a given thin section. The highest biotite content is found in the tonalitic gneisses, averaging 13%. The biotite is usually brown though in some instances dark green (e.g., in 3151-1A, a biotite-granodiorite gneiss); it is often kink-banded (Fig. 4b) and in some cases poikilitic. The biotite is primary while the chlorite is usually considered to be a secondary or alteration mineral; the biotite may be partly or wholly replaced by chlorite. The chlorite is found along the (001) planes of the biotite or as complete replacements of biotite. In one sample (5234-5, an altered granodiorite gneiss) apparently all of the biotite has been altered to chlorite, yielding an unusually high 16% chlorite content; the chlorite averages 2% down to trace amounts in the gneisses.

Chloritization does not solely affect biotite, nor is the product of biotite alteration always chlorite. Chlorite may be found replacing sericitized alternate twin sets in plagioclase (e.g., in 2600-3, a granite gneiss). Sometimes chlorite is found associated with partly altered opaques or epidote, or as a secondary mineral in amphibole. In another sample (5980-1, a granite gneiss), much of the biotite is strongly altered to muscovite and/or talc plus opaques.

The biotite in some cases appears to be intimately associated with other minerals in a vermicular or symplectic intergrowth. It is found marginally intergrown with plagioclase in several samples (e.g., in 4896-2a, a granite gneiss, and in 4892-1b1-mafic and 5234-10, both biotite-tonalite gneisses). Biotite may also be intergrown with amphibole (e.g., in 7103-1i, a biotite-hornblende-tonalite gneiss).

Calcite and muscovite or sericite occur as alteration products or as "free" grains and in fractures. They tend to concentrate near fractures although in many samples there is no notable heterogeneity in their distribution. Chloritization also notably increases towards fractures or lithologic contacts as in 5985-5b, 5c, in which a hornblende-mica-plagioclase schist is in contact with a biotite-granodiorite gneiss.

Muscovite or sericite, usually subhedral, is commonly present in altered plagioclase, although sometimes it forms in biotite or chlorite parallel to (001), or in conjunction with the alteration of opaques and other mafic minerals. It may also be intergranular; in such cases plagioclase sericitization proceeds from the grain boundaries toward the core.

The calcite is almost always anhedral, although there is euhedral calcite in 6153-4c, a leucocratic granodiorite gneiss. The calcite more often occurs as "free" grains or as a vein-filling than as a specific alteration product.

Other minerals - opaques, epidote, apatite, sphene, zircon, amphibole, allanite, rutile, garnet - usually occur as rather evenly disseminated accessory minerals whose average abundances range from less than 0.10% up to 1%. Notable exceptions are 7% epidote in 5234-5, an altered granodiorite gneiss, 3% opaques in 3151-5A, a biotite-granodiorite gneiss, and 13% amphibole in 7103-1i, a biotite-hornblende-tonalite gneiss. In some cases zircon (e.g., in 5492-1d1,1d2, a monzogranite gneiss), epidote, sphene, or apatite are found clustered or inhomogeneously distributed in a given thin section, yielding locally high abundances of these minerals.

Opaque minerals are most abundant in the granodioritic and monzogranitic gneisses, totaling about 1%, twice as much as in the gneisses of tonalitic composition. Magnetite or titanomagnetite and its common alteration product, leucoxene, are the most prevalent opaques. Secondary hematite is less common. Rare, mostly subhedral to anhedral pyrite (euhedral in 6155-26, a granodiorite gneiss) may also be present. The magnetite is anhedral to subhedral and generally quite fine-grained although in 3696-1.1b (a monzogranite gneiss) it is almost 5.5 mm across, and more than 1-mm-diam magnetite is found in 5240-1A, a biotite-granodiorite gneiss.

Alteration of magnetite to leucoxene and/or hematite is usually concentrated at the rim or along partings in the magnetite, although whole grains may be altered. Occasionally associated with the opaques are poikilitic inclusions of pyrite, epidote, chlorite, sphene, muscovite, or other felsic minerals (e.g., in 5240-1A, a biotite-granodiorite gneiss) and rims of epidote or saussurite and/or sphene. Some indeterminate granular pseudomorphs, apparently replacing opaques, are found in the granite gneisses 2844-2 and 3694-1.1. Rarely the magnetite exhibits pleochroic haloes, indicative of the presence of appreciable uranium (e.g., in 2600-3, a monzogranite gneiss, and in 3151-5A, a biotite-granodiorite gneiss.

In some instances small grains of magnetite are associated with biotite or chlorite or altered sphene (usually replaced by leucoxene). Sagenitic rutile is present in chlorite in a biotite-granodiorite gneiss, 5234-11a.

The epidote in the gneisses is usually pleochroic green/yellow but in some cases, probably the iron-free variety clinozoisite, it is nonpleochroic and exhibits anomalous birefringence. The epidote ranges from anhedral grains or stringers to euhedral crystals. It may rim or be intimately associated with other minerals: in 2600-3, a monzogranite gneiss, epidote surrounds opaques or rarely biotite, and in 5234-10, a biotite-tonalite gneiss, it rims or is associated with biotite, chlorite, or opaques. Occasionally the epidote is surrounded by a granular rim, which may be saussuritic (e.g., in 4893-1a, a biotite-tonalite gneiss). In some samples pleochroic haloes, apparently due to high uranium contents, surround various accessories including epidote or saussurite (e.g., in 5234-10, a biotite-tonalite gneiss).

Common epidote, as against the iron-free clinozoisite, is an invariable associate of allanite where the latter is present (e.g., in 4893-1a, a biotite-tonalite gneiss, or in 5240-1B, a monzogranite gneiss). Allanite, another epidote group mineral, is usually dark brown, subhedral to euhedral, and zoned, with the main axis of the surrounding epidote apparently inclined to that of its host.

The amphibole in the gneisses, possibly hornblende, is usually brown or pleochroic green/yellow, and may be zoned. It is usually subhedral to euhedral, but it may be anhedral. In some cases the amphibole is interstitial (e.g., in 7103-1i, a biotite-amphibole-tonalite gneiss) or in optically continuous, poikilitic plates, measuring up to 2.9 by 1.5 mm in 5234-10, a biotite-tonalite gneiss. The amphibole usually exhibits good cleavage (e.g., in 5234-10, a biotite-tonalite gneiss). In some gneisses the amphibole is altered along its cleavages to chlorite or biotite (e.g., in 5240-1A, a biotite-granodiorite gneiss, or in 7103-1i, a biotite-amphibole-tonalite gneiss).

Zircon is the most abundant of the remaining trace minerals; it is subhedral to euhedral and may have pleochroic haloes, related to high uranium content (Fig. 6).

Apatite and sphene are usually present in trace amounts. The apatite is subhedral to euhedral, minute and ubiquitous. In the tonalite gneisses the apatite is often included in the plagioclase. Sometimes the apatite is enclosed within small mutually aligned rectangular patches of contrasting relief, possibly incipient antiperthite exsolution, in the plagioclase.

The sphene is usually anhedral to subhedral in the gneisses. Sometimes the sphene is associated with epidote and/or the sphene has rims of leucoxene. Both

Fig. 6. Pleochroic halo surrounding zircon in biotite, in biotite-granodiorite gneiss from the 960-m (3151-ft) depth in GT-2; plane light. (Bar equals 0.5 mm).

sphene and apatite may have pleochroic haloes indicative of high uranium contents.

Rutile and garnet are rare accessories in the gneisses. Where present the rutile is usually sagenitic, forming as needles along rational planes in biotite or chlorite. The garnet is pink, of undetermined composition, and is found in only one of the major gneisses, 5487-M-1, a monzogranite gneiss.

2. Schistose Rocks. The mafic metamorphic rocks are mainly schistose rocks whose major constituents are plagioclase, amphibole (ferrohastingsite), biotite and quartz (see Tables III and IV). In one sample muscovite is a major mineral. There is also an unusual zone of magnetite folia in monzogranitic gneiss. All of the mafic rocks sampled occur within a 500-ft interval, although drill cuttings and spectral gamma logs indicate that they occur throughout a 2000-ft vertical section.

The unique zone of mafic folia is quite heterogeneous in mineral distribution and textures. There is an unusual concentration of magnetite in this zone, with small amounts of pyrite, chalcopyrite, hematite and pyrrhotite. The complex ore petrography requires further study before a detailed description can be made. The gangue minerals are mostly quartz and feldspar, with minor mica, and accessories and alteration products such as calcite, epidote, apatite, zircon,and amphibole.

There are both textural and mineralogical differences among the schistose rocks. Their textures vary in the predominance of schistose versus granoblastic fabric, and in the degree of metamorphic differentiation and development of porphyroblasts. One of the mafic rocks cored (5983-3b) is an amphibolite with only limited schistosity. Its texture is granoblastic, equigranular and homogeneous except for occasional porphyroblasts; there is only a faint foliation detectable. The other mafic rocks (56542b, 5980-2b, 5985-5c) sampled are quite schistose with some porphyroblasts and some felsic/mafic segregation banding. The porphyroblasts usually occur as clusters, often monomineralic, of plagioclase feldspar and/or quartz and/or ferrohastingsite.

Grain size varies within a given sample as well as among the schists. There is usually a notable hiatus in grain size between the main fabric and the porphyroblasts in each of these rocks. In 5654-2b (a ferrohastingsite-biotite-plagioclase schist) there is a continuous range of grain size from fine- to medium-grained, whereas 5980-2b,2c (a quartzo-feldspathic biotite-ferrohastingsite schist), 5983-3b (an amphibolite) and the mafic portion of 5985-5b,5c (a ferrohastingsite-mica-plagioclase schist), are essentally fine-grained and equigranular with medium-grained porphyroblasts.

Plagioclase averaging An_{36}, the most abundant felsic mineral in the schists and amphibolite, ranges from very fresh, with only incipient sericitization, to completely altered. The highly altered plagioclase is often confined to the porphyroblastic feldspar and the feldspar near veins (e.g., in 5985-5b,5c-mafic). Although in most samples it is twinned, much of the plagioclase in 5983-3b is untwinned. The plagioclase is sometimes poikilitic, enclosing amphibole, biotite and quartz (e.g., in 5985-5b,5c-mafic). In 5983-3b there are poikilitic megacrysts of plagioclase enclosing biotite laths and apatite. Rarely, the feldspar contains antiperthite as mutually oriented rectangular patches (e.g., in 5980-2b,2c).

The porphyroblasts and felsic segregation bands exhibit potentially significant textures. In rare polymineralic porphyroblasts, plagioclase has nucleated at quartz triple points (e.g., in 5980-2b, 2c); also quartz appears at plagioclase triple points in porphyroblasts (e.g., in 5654-2b, 2c). Monomineralic porphyroblasts are usually granoblastic or granoblastic-polygonal aggregates, elongate in the direction of schistosity.

The quartz and rare potassium feldspar are anhedral and fresh. The quartz is often porphyroblastic, with sutured grain boundaries or triple points, and mosaic extinction resembling grid twinning. The potassium feldspar is usually interstitial in the groundmass, although it may occur as antiperthitic patches in plagioclase.

The major mafic minerals in the schistose rocks are biotite and amphibole. The amphibole is ferrohastingsite and is usually pleochroic green/brown/light brown. Euhedral to anhedral, it is often altered along cleavages to calcite, muscovite, chlorite, and/or talc (e.g., in 5980-2b, 2c and 5985-5b, 5c-mafic; see Fig. 7). Ferrohastingsite has been largely replaced by calcite near the fracture in 5985-5b, 5c-mafic. There is no evidence of reaction between ferrohastingsite and biotite. The biotite is slightly more concentrated parallel to the fracture in 5985-5b, 5c-mafic; otherwise the biotite is ubiquitous. The biotite content is low (2%) in the amphibolite (5983-3b) compared with the 12-29% in the three schist samples. The biotite is subhedral or euhedral and brown; some is poikilitic, enclosing zircon (e.g., in 5980-2b, 2c) or epidote (e.g., in 5654-2b), although usually it is free from inclusions. The biotite may rarely exhibit vermicular intergrowth with plagioclase (e.g., in 5654-2b).

Chlorite is a rare alteration product of biotite in the mafic schists and amphibolite, never exceeding trace amounts. Calcite and muscovite are somewhat more common. These two minerals are very abundant in 5985-5b, 5c-mafic, owing to the major fracture along the boundary with the next lithologic unit, granodiorite gneiss, 5985-5b, 5c-felsic. In 5985-5b, 5c-mafic, the calcite forms strain shadows behind amphibole and also occurs as discrete grains.

Epidote is a fairly common accessory mineral. It usually occurs as independent subhedral grains but it may occur as saussurite or as inclusions or reaction rims. Surrounded by pleochroic haloes, it is poikilitically enclosed in biotite in 5654-2b. Where allanite is present, epidote invariably rims it; in 5654-2b the associated epidote is euhedral, with irregular allanite centers. The allanite may be zoned (e.g., in 5654-2b).

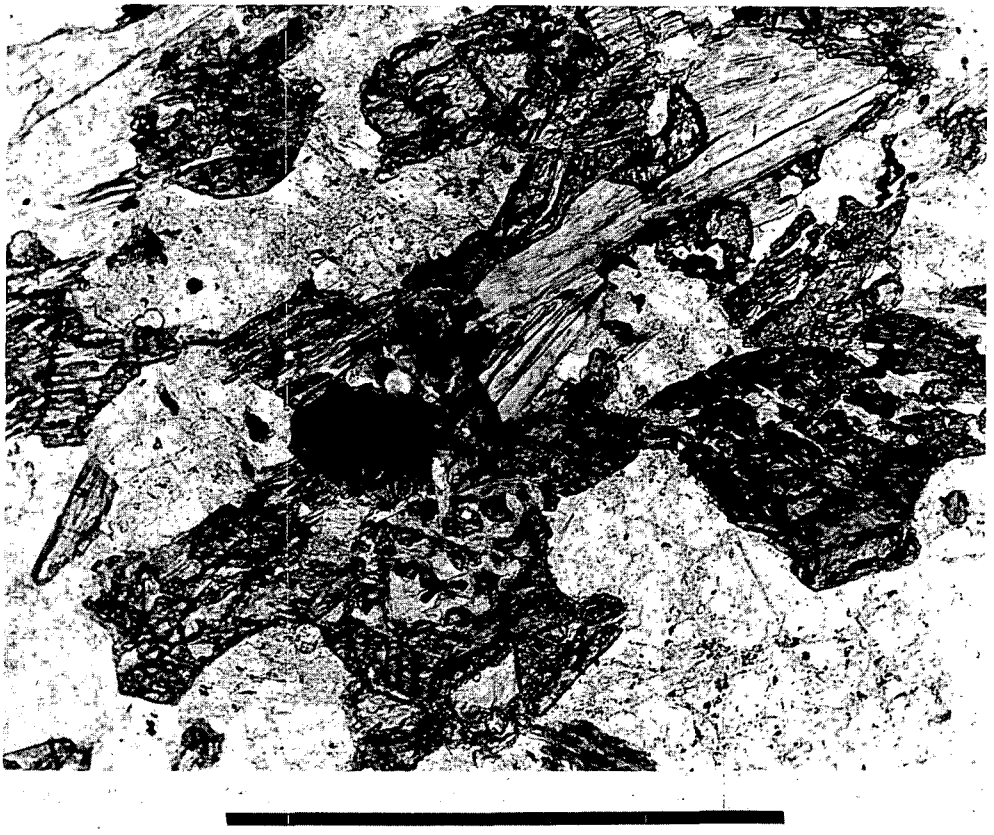

Fig. 7. Euhedral amphibole altered along cleavages to chlorite or talc, in mafic schist from the 1824-m (5985-ft) depth in GT-2; plane light. (Bar equals 0.5 mm).

There are minor amounts of apatite, zircon, sphene, and opaque minerals in the schistose rocks. The zircon in 5980-2b, 2c has notable pleochroic haloes where it is enclosed in biotite. The opaque minerals--magnetite, leucoxene, hematite, pyrite-- are usually present only in trace amounts. In 5654-2b the pyrite appears to be prismatic and is enclosed in biotite.

3. Granitoid Rocks. The granitoid rocks are confined to two 50-ft-thick leucocratic monzogranite dikes or sills, one of which was cored, and an extensive biotite-granodiorite body, which was drilled for more than 335 m (1100 ft) in GT-2. This latter body is apparently a pluton whose emplacement was contemporaneous with that of the granite dikes or sills at shallower levels.

The leucocratic monzogranite dike or sill cut at the 1295.4-to 1310.6-m (4250-to 4300-ft) level is essentially homogeneous and hypidiomorphic- to allotriomorphic-granular with no or very minor foliation or lineation evident

either megascopically or microscopically. Besides having a granitoid texture, the granite differs from the gneisses most notably in plagioclase alteration and other secondary features. The individual minerals of the granitoid monzogranite and the monzogranitic gneisses are essentially similar in character. The plagioclase in both is sericitized, but only in the dike or sill (4282-4, leucocratic monzogranite) does the mica form parallel to the twin plane as well as at an angle to (010) of the host. In the granite calcite may be present as alteration of the core of plagioclase grains (4282-4), especially adjacent to the mineralized fractures (see Section V.A). Also in 4282-4), triple points, suggestive of recrystallization, characterize the contact relations between quartz grains.

In the same monzogranite body epidote rims or is associated with chlorite. The chlorite takes different forms from subhedral to anhedral, and it may be in radiating clusters. The opaques are in some cases fragmented and expanded by secondary mineralization, usually chlorite (e.g., in 4282-4).

Although the monzogranite is generally rather fine-grained, there is biotite as coarse as 2 mm in length (in 4279-2), and 1.5-mm-diam myrmekite (in 4279-2 and 4280). Muscovite and apatite are also coarser than in the gneisses.

Within the biotite-granodiorite pluton entered at about 2591 m (8500 ft) in GT-2, there are minor felsic segregations of monzogranite composition (e.g., 9521-1). The gneissic unit of biotite granodioritic composition cored at 2928.2 - 2928.8 m (9607-9609 ft) has certain characteristics in common with the major granitoid biotite-granodiorite body; these features are primarily apparent petrographically and megascopically. Microscopically, the mineral habits and textures are similar, and in hand specimen, the lower unit would appear to represent a locally foliated zone in the biotite granodiorite. However, chemical and modal analyses suggest that these are lithologically distinct units.

The modes of these granitoid versus gneissic biotite granodiorites differ considerably in their major felsic constituents. The granitoid body contains 10% more microcline on the average, whereas the gneissic unit has 9% more plagioclase and 5% more quartz in its average mode. Both contain 12% biotite. The minor minerals differ insignificantly; epidote and sphene are high in both, averaging 2% in the granitoid body and 1% in the gneissic unit. Garnet, not found in the granitoid section, is found in the biotite-granodiorite gneiss (e.g., 9607-2A, 2B).

The major differences in texture between these granitoid and gneissic rocks of biotite-granodiorite composition are in grain size and shape. The granitoid biotite granodiorite is generally finer grained than the gneiss. The latter is quite variable in grain size; it contains grains of more than 3-mm length down to very fine-grained crystals. The larger grains are usually subhedral plagioclase although quartz may be in optical continuity over a much larger area, probably as a result of mineral segregation into felsic and mafic bands.

The felsic minerals are similar in the granitoid and gneissic samples, except that the plagioclase is generally much fresher in the gneiss. In both cases the plagioclase is subhedral while the K-feldspar and quartz are anhedral with irregular or sutured contacts. The alkali feldspar tends to be clustered, as does the quartz, or the microcline may be interstitial to the plagioclase. Where the plagioclase is altered, it is usually totally sericitized, or partly altered from the perimeter inward. Perthite is rare in both the granitoid and gneissic samples; it occurs as short stringers, rectangular patches, or irregular blebs.

The epidote, sphene and opaques tend to be concentrated in the biotite-rich bands in the gneiss, but evenly distributed in the granitoid samples. The biotite, which is dark green, tends to be more subhedral in the foliated rocks, whereas the granitoid samples have more anhedral, interstitial biotite. The biotite poikilitically includes euhedral apatite in the granitoid body, and encloses epidote, zircon, and apatite in the gneiss. There are no pleochroic haloes in either case.

The abundant sphene is of somewhat different character in the granitoid compared with the gneissic samples. In the granitoid biotite granodiorite, it is generally subhedral to euhedral, whereas in the gneiss it is usually subhedral to anhedral. In the former it usually occurs as integral unaltered grains, while in the gneiss many sphene crystals appear to be crushed or fragmented, essentially in place, and in many cases largely replaced by opaques (Fig. 8). In the gneiss, the opaques are anhedral, often having embayed contacts with the sphene. The opaques seem to have replaced the sphene from the interior towards the perimeter of the grains; in some cases only a narrow continuous rim of sphene, anhedral in outline, surrounds the opaques. In the granitoid samples the opaques are often but not necessarily associated with the sphene; if the sphene encloses opaques, the latter tend to be angular and anhedral or euhedral, suggesting a poikilitic relationship rather than one of replacement. The

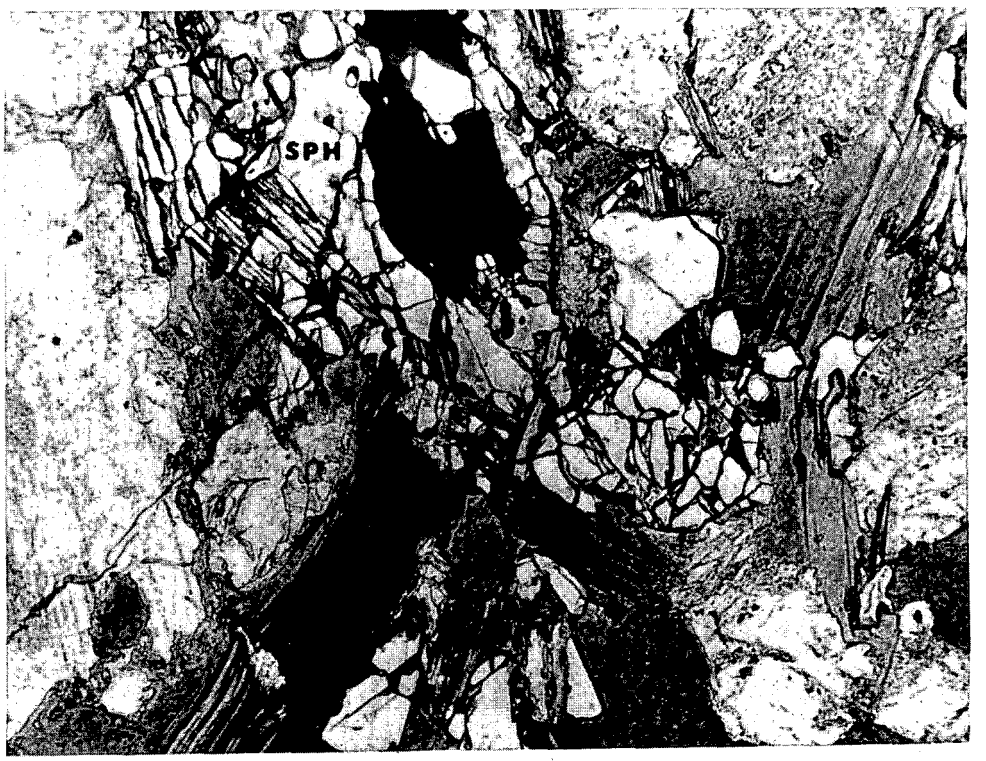

Fig. 8. Fragmented sphene (SPH), in gneissic biotite-granodiorite from the 2928-m (9607-ft) depth in GT-2; plane light. (Bar equals 1 mm).

sphenes in both the granitoid and gneissic samples do tend to be poikilitic, enclosing apatite, other felsic minerals, and epidote as well as opaques.

The zircons are more euhedral and have more pronounced zoning in the gneiss than in the granitoid samples. The zones are in some cases notably truncated by the perimeters of the grains.

Epidote is generally anhedral in the granitoid biotite granodiorite. In the gneiss it is usually anhedral but may be subhedral, and may be poikilitic, enclosing biotite for example.

Garnet, which apparently occurs only in the gneissic biotite granodiorite, may be pink and translucent (e.g., in 9607-M1) or colorless and transparent (e.g. 9607-2B).

The other accessories or alteration products in these rocks are euhedral apatite, subhedral to anhedral muscovite or sericite, and anhedral calcite.

C. CHEMISTRY

Whole-rock chemical analyses were performed on 38 samples of the Precambrian rocks from GT-2 and two samples from EE-1. The results of these analyses are presented in Table V with the calculated norms. Average rock compositions for units distinguished above on the basis of petrographic and other evidence are reported in Table VI. Chemical data is presented graphically in Fig. 9.

Large chemical differences are apparent in the reported results. These differences are perhaps best shown in a frequency distribution of SiO_2 contents (Fig. 9a). This figure shows a roughly trimodal distribution of SiO_2 contents. The lowest SiO_2 contents (55 to 56%) are from the ferrohastingsite-biotite schists. These values are separated by a broad gap from the peak extending from 62 to 70% SiO_2. This second group consists of samples of the biotite granodiorite from the bottom of GT-2 and a number of biotite granodioritic and biotite tonalitic gneisses. A third major group extends from 71 to 78% SiO_2 and consists of samples of the monzogranite dike or sill, one pegmatite, a felsic segregation from the biotite granodiorite and various leucocratic monzogranitic gneisses. Rock chemistries will be discussed below according to the same system applied to the petrography.

The two granitoid rock units distinguished megascopically and on the basis of petrographic and spectral gamma evidence also have distinctive chemical compositions. Whole-rock chemical analyses were performed on three samples from the leucocratic monzogranite body (Core 10) encountered at 1295.4 to 1310.6 m. As may be seen from Tables V and VI this rock is chemically homogeneous and is characterized by a relatively high SiO_2 content and low Fe_2O_3, FeO, and MgO contents.

The biotite granodiorite sampled by Cores 24, 25, and 26 is also a very homogeneous rock. With the exception of very minor felsic segregations such as sample 9521-M1 this unit is characterized by a low SiO_2 content (62 to 66%). When this unit is compared to other GT-2 rocks with similar SiO_2 contents, the TiO_2, Fe_2O_3, FeO, K_2O, P_2O_5 and SrO are strikingly high. The high Fe_2O_3, FeO, and K_2O contents are reflected in the high modal biotite content while the high TiO_2 and P_2O_5 can be accounted for by high sphene and apatite contents, respectively.

Figure 9b illustrates a Harker diagram of the biotite granodiorite with one sample of a biotite-granodiorite gneiss with a similar SiO_2 content included for

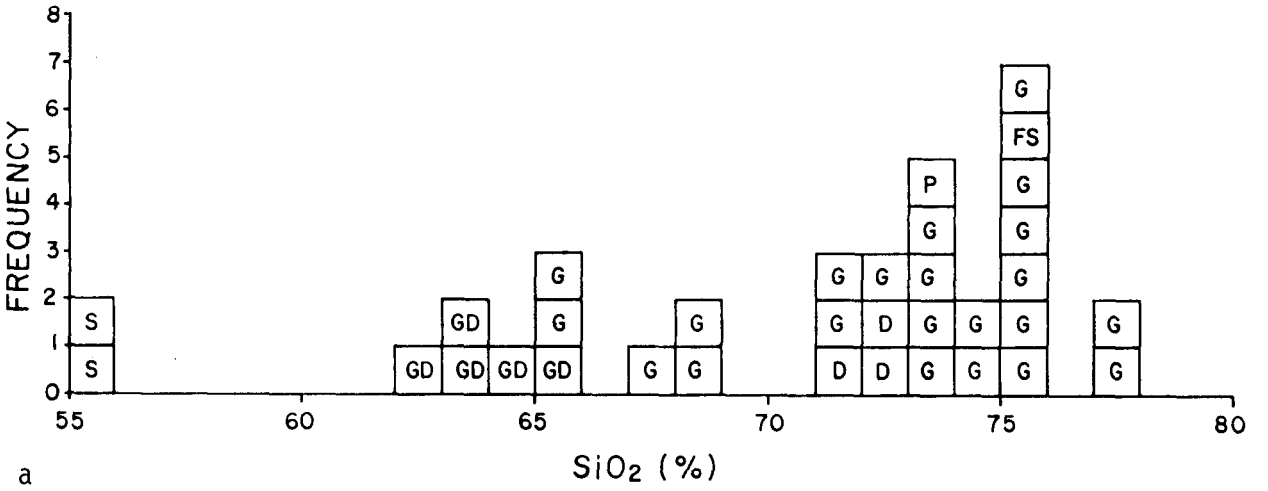

a

Fig. 9. Chemical variations in GT-2 and EE-1 rocks.

a. (Above) Frequency distribution of SiO_2 contents in Precambrian rocks from GT-2 and EE-1.

Key: S - Mafic schist
GD - Biotite granodiorite
D - Leucocratic monzogranite dike
P - Pegmatite
FS - Felsic segregation in biotite granodiorite
G - Gneiss

b. (Right) Harker diagram for biotite granodiorite. Symbols not connected by lines represent a biotite-granodiorite gneiss included for comparison purposes.

comparison. It is apparent from this diagram that this rock is relatively homogeneous and considerably different from the biotite granodioritic gneisses. As would be expected, the diagram also shows a decrease in MgO and TiO_2 contents with increasing SiO_2.

The foliated metamorphic rocks from GT-2 and EE-1 are extremely variable in chemical composition. Even if the analyses of the magnetite folia (5492-M1) and the ferrohastingsite-biotite schists (5654-1 and 5654-2b, c) are excluded, the SiO_2 content of the remaining gneissic rocks ranges from about 62 to 77%. The variation in other oxides, especially K_2O, is also large.

The banding prominent in some sections of the core leads to large chemical differences in distances as short as a few centimeters. Samples 7103-A, -1E,

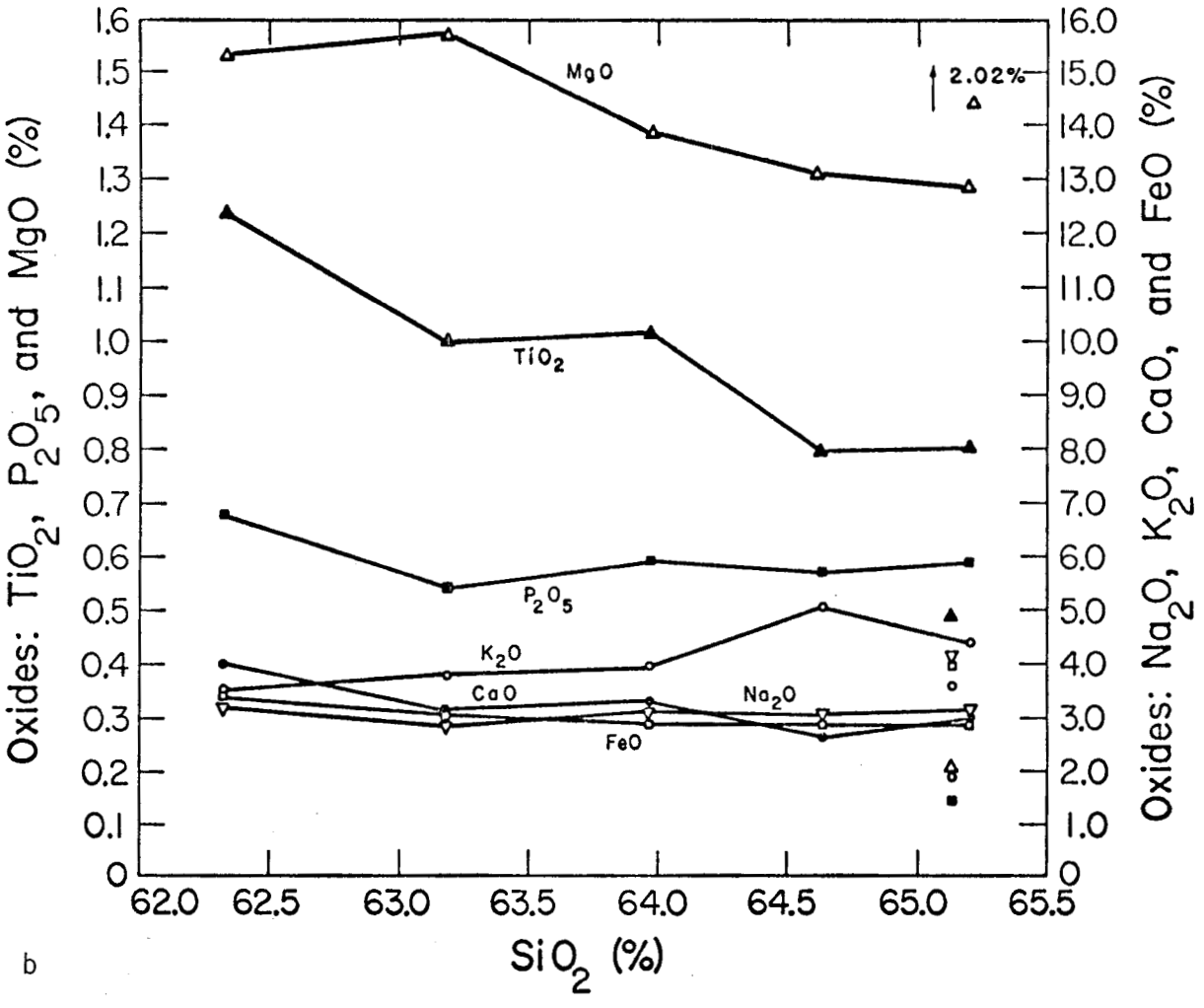

b

and -1H were collected by drilling 2-cm-diam cores from a single short section of a large Christiansen diamond core. These small cores sampled different layers in a banded gneiss which had grossly different chemical compositions. For example, the SiO_2 contents of these three samples ranged from 65 to 75% with similar variations in the other oxides. Thus, almost the entire spread in composition of the felsic to intermediate rocks may be found over short distances in the core. Such variations are common in the gneissic rocks. With a single exception among the gneisses sampled, alumina contents are sufficiently high to cause the rocks to be corundum normative. This may suggest a sedimentary origin for the gneisses.

The results of two analyses of the ferrohastingsite-biotite schist are presented in Table V. The two analyses agree closely, confirming the homogeneous nature of this unit indicated by both petrographic study and spectral gamma logging. This rock has relatively high K_2O, TiO_2,and P_2O_5 contents. It

is hypersthene-normative and closely resembles an andesite in composition (Table VII).

VI. GEOTHERMAL IMPLICATIONS

All cores examined show evidence of extensive natural fracturing and rock alteration with an expected positive correlation between fracture frequency and degree of alteration. The fractures occur in several sets and a variety of orientations, but generally are either horizontal, vertical, or steeply inclined (dip of about 60°). They are commonly on the order of 8 cm apart, occasionally as close together as 1 cm. They are usually well sealed by secondary minerals deposited from the hydrothermal fluids that once circulated through them (Fig. 10). This suggests that in spite of the large population of natural fractures, the overall permeability of the rock should be low. This has been

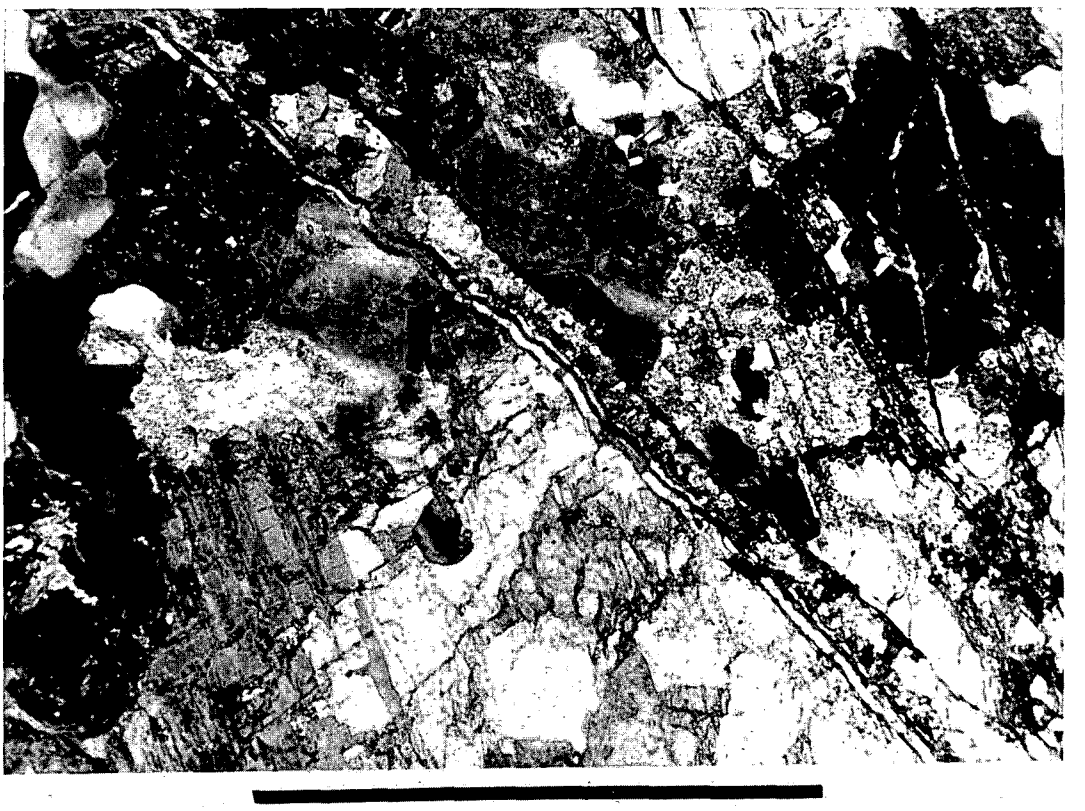

Fig. 10. Calcite-filled fracture showing more than one stage of fracture filling, in biotite-granodiorite gneiss from the 960-m (3151-ft) depth in GT-2; crossed nicols. (Bar equals 1 mm).

verified both in laboratory tests on core samples and in the field by pressurizing the boreholes to produce hydraulic fractures.[17] It also suggests, since the principal secondary mineral is calcite, that an acid leaching treatment might be used to increase permeability locally by reopening preexisting fractures.

Associated with sealed fractures through which hydrothermal fluids once flowed, zones of rock alteration are regions with physical, chemical, and mechanical properties significantly different from those of the unaltered rock around them. The clay found in a few of the fractures — notably in one prominent vertical fracture that strikes about N60°E in the interval 1672-1674 m — is a finely divided alteration product of adjacent feldspars. Washing it out might reopen the natural fractures sufficiently to permit fluid flow through them, which could create flow passages through the rock mass between parallel hydraulic fractures. On the other hand, the accumulation of clays elsewhere (or alteration of feldspars on fracture surfaces) might plug hydraulic fractures or their connections to boreholes. This may partly explain the behavior of certain hydraulic fractures made through casing perforations, which appeared to close and reseal during periods when flow through them was not maintained.

Fracture-filling secondary minerals, especially calcite, are relatively weak in tension and shear. For example, at 5-kb confining pressure, 200°C, and a strain rate of about 10^{-4}/s, a stress of only 28 bars is sufficient to cause translational twinning in calcite.[18] A more realistic confining pressure (800 bars) would lower this value. Filling variously oriented closely spaced fractures, the low-strength calcite should have a profound effect upon the behavior of the reservoir rock. The filled fractures would be expected to serve as effective "starter cracks" where fracturing of the rock could be initiated at relatively low stress. This probably explains both the low pumping pressures at which hydraulic fractures are produced in the Fenton Hill boreholes and the absence of a sudden "breakdown" when fracturing begins. The low stress required to induce translational twinning in calcite would promote readjustment along the filled fractures (Fig. 5b). This would contribute to both propping and pinching off of the fractures. Seismic energy may be released during twinning, which could account for some of the seismic noise recorded during fracturing and reinflation.

The foliated structures of the banded gneisses and schists are results of inhomogeneous deformations during metamorphism from what were likely very

ancient sediments[19] with physically and chemically distinct layers. This relict anisotropy of rock properties would be reinforced by the chemical and mineralogical segregation that has accompanied subsequent recrystallization. Thus in the metamorphic rocks there are alternating light and dark bands with differing physical properties; these narrow zones tend to be steeply inclined, though not vertical. The associated anisotropy of strength is probably insufficient to compensate for large differences in principal stresses that may exist in deeply buried rock. Thus it would not be expected to cause a hydraulic fracture to deviate significantly from the vertical. At Fenton Hill where the two horizontal principal stresses do not differ greatly the fracture may curve in the horizontal plane, following the convolutions of the foliated rock structure.

It appears unlikely that the inherent anisotropy of elastic properties, and therefore of wave velocities, would be sufficient to have a significant effect on acoustic measurements of distance and direction in these metamorphic rocks. In comparison, strong reflection and refraction effects are expected at contacts between dissimilar rock types, particularly when a major fracture occurs at such a contact. Such is the case at the 1824-m depth in GT-2 where mafic schist is in fault contact with a granodioritic gneiss.

The mineralogical contrast between adjacent mafic and felsic layers in the strongly banded rocks comprising most of the Precambrian section has implications for chemical leaching. In particular, the high concentration of quartz (up to about 47%) in the felsic bands, and its recrystallization into connected clusters of coarse grains, may facilitate channeling when the quartz is attacked by a leaching solution such as sodium carbonate. This channeling, which would increase permeability, is less likely to occur in the igneous intrusives with essentially isotropic textures or less abundant quartz (about 25 to 35%). This may partially explain the abortive attempt to increase the permeability of the igneous rock near the bottom of the section by leaching it with a dilute sodium-carbonate solution. The leaching might have succeeded in the metamorphic rock higher in the section, where the quartz tends to be interconnected.

The occurrence of small crystals at triple points in a previously recrystallized structure, together with geochronological evidence,[20,21,22] indicates that these rocks have undergone more than one cycle of deformation and intense heating. One episode of heating undoubtedly accompanied emplacement of the igneous intrusives described above. Another probably occurred during ascent of

the magma body responsible for formation of the nearby Valles Caldera. These and perhaps other intense thermal events represent a very complex history of heat flow in several nonvertical directions.

Evidence for stress accumulation and crustal deformation since the last major thermal event in the area includes bent crystal lattices in plagioclase (Fig. 4a), kink-banding in biotite (Fig. 4b, c), twinning in calcite, and occasional crushing and fracturing of sphene (Fig. 8), amphibole and quartz crystals. This accumulation of tectonic stresses is a major factor in controlling the orientation of hydraulic fractures produced from GT-2 and EE-1.

The types and distribution of certain minerals in the Precambrian core samples are of particular interest to the geothermal project. (1) The abundant quartz in these rocks, as discussed above, explains the very low penetration rates and rapid wear of the diamond core bits. It also accounts for the high rate of erosive gauge wear observed when air was used as the circulating medium while drilling with carbide-insert bits. (2) The widespread and inhomogeneously distributed mica and chlorite partially explain the relative ease with which these rocks crush under the localized pressure of a hard button on the carbide-insert drilling bits. Hence these bits have relatively high penetration rates and long bit life when used for both conventional drilling and coring. (3) The appearance of fluoride ion in high concentrations in water circulated through these rocks is in part explained by the presence of hydroxyl-bearing minerals, i.e., apatite and biotite, in which fluorine substitutes for the hydroxyl ion. Fluoride ion may also have been contributed by very small amounts of fluorite observed in some fractures. Fluoride adsorbed on grain boundaries may also have been released by the leaching. (4) The pleochroic haloes (Fig. 6) around grains of magnetite, epidote, saussurite, zircon, sphene, and apatite in the metamorphic rocks indicate the presence in these minerals of relatively high concentrations of uranium, some of which might conceivably be recovered by leaching as a by-product of a heat-extraction system. In the igneous rocks the absence of such haloes suggests that significant concentrations of uranium will be found only in or adsorbed on secondary minerals filling fractures. This is at least in part confirmed by the results of spectral gamma logging,[23] which show very narrow zones of high uranium content coincident with fractures. (5) The presence of magnetite has made it possible to orient otherwise unoriented cores and core fragments on the basis of paleomagnetism. However, the remanent magnetism has had a deleterious effect on the downhole

orienting devices. The orientation of the paleomagnetic field retained in the magnetite differs significantly from that of the earth's present magnetic field, and thus causes deflection of the compass needle used in any downhole magnetic surveying tools. The compass deflection is proportional to the local magnetite concentration, which is observed to vary widely in the metamorphic rocks from the Fenton Hill boreholes. This adds significantly to the uncertainties of magnetic hole surveys, drilling-tool guidance, and magnetic determinations of the orientations of downhole instruments and equipment.

The demonstrated chemical homogeneity of the biotite granodiorite in which the HDR experiments are being conducted is important as it greatly simplifies problems of predicting rock-water interaction. In contrast to the banded gneiss/schist complex with its extreme chemical variations, the granodiorite reservoir may be represented by a single starting rock composition, thus reducing experimental work necessary for duplication of the reactions.

VII. SUMMARY

The Precambrian basement rocks at the LASL Fenton Hill site consist of a complex sequence of chemically and mineralogically heterogeneous gneisses, schist, and amphibolite intruded by several relatively homogeneous igneous rocks. These igneous rocks include thin dikes or sills of leucocratic monzogranite and an intrusive biotite-granodiorite body near the bottom of the section.

The Precambrian granitic rocks are composed primarily of four common rock-forming minerals: quartz, plagioclase, potassium feldspar, and biotite. Petrographic analysis indicates that despite the relative simplicity of the mineralogy, abundances of the four main minerals vary considerably at different levels in the geologic section. This produces large variations in the whole-rock chemistry of the samples. Fortunately for the LASL geothermal program, there is little variability in mineralogy or chemistry within the biotite-granodiorite body in which the present experiments are being conducted.

Mineral alteration, such as biotite to chlorite, and plagioclase to sericite and calcite, is evident throughout the Precambrian section. This reflects multiple past thermal events and the numerous fractures along which hydrothermal fluids have moved. Calcite produced during the alteration of plagioclase also seals the abundant fractures, yielding an essentially impermeable reservoir rock. Because this fracture-filling calcite is easily dissolved, it may be removed by acid leaching to increase permeability. The low

shear strength of the calcite suggests that movement may occur along the fractures and produce seismic signals.

While this study has produced a number of useful observations and explanations, its most important conclusion is that at Fenton Hill there exists at depth a large, essentially equigranular, homogeneous intrusive body of biotite granodiorite, within which all natural fractures have been effectively sealed. This provides a nearly ideal environment for development and testing of the LASL hot dry rock geothermal energy concept.

REFERENCES

1. M. C. Smith, "Geothermal Energy," Los Alamos Scientific Laboratory Report LA-5289-MS (May 1973).

2. F. G. West, P. R. Kintzinger, and A. W. Laughlin, "Geophysical Logging in Los Alamos Scientific Laboratory Geothermal Test Hole No. 2," Los Alamos Scientific Laboratory Report LA-6112-MS (November 1975).

3. R. L. Smith, R. A. Bailey, and C. S. Ross, "Structural Evolution of the Valles Caldera, New Mexico, and Its Bearing on Emplacement of Ring Dikes," U.S. Geol. Survey Prof. Paper 424-D (1961).

4. R. L. Smith, R. A. Bailey, and C. S. Ross, "Geologic Map of the Jemez Mountains, New Mexico," U.S. Geol. Survey Misc. Geol. Inv. Map I-571 (1970).

5. R. L. Smith and R. A. Bailey, "The Bandelier Tuff: A Study of Ash-Flow Eruption Cycles from Zoned Magma Chambers," Bull. Volcanologique 29, 83-104 (1966).

6. C. S. Ross, R. L. Smith, and R. A. Bailey, "Outline of Geology of the Jemez Mountains, New Mexico," New Mexico Geol. Soc. Twelfth Field Conf., Albuquerque Country (1961).

7. R. A. Bailey, R. L. Smith, and C. S. Ross, "Stratigraphic Nomenclature of the Volcanic Rocks in the Jemez Mountains, New Mexico," U.S. Geol. Survey Bull. 1274-P (1969).

8. R. R. Doell, G. B. Dalrymple, R. L. Smith, and R. A. Bailey, "Paleomagnetism, Potassium - Argon Ages, and Geology of the Rhyolites and Associated Rocks of the Valles Caldera, New Mexico," Geol. Soc. Am. Mem. 116, pp 211-248 (1968).

9. W. D. Purtyman, "Geology of the Jemez Plateau West of the Valles Caldera," Los Alamos Scientific Laboratory Report LA-5124-MS (1973).

10. F. G. West, "Regional Geology and Geophysics of the Jemez Mountains," Los Alamos Scientific Laboratory Report LA-5362-MS (August 1973).

11. W. D. Purtymun, F. G. West, and R. A. Pettitt, "Geology of Geothermal Test Hole GT-2 Fenton Hill Site, July 1974," Los Alamos Scientific Laboratory Report LA-5780-MS (November 1974).

12. P. C. Perkins, "Petrology of Some Rock Types of the Precambrian Basement Near the Los Alamos Scientific Laboratory Geothermal Test Site, Jemez Mountains, New Mexico," Los Alamos Scientific Laboratory Report LA-5129 (1973).

13. H. R. Duchene, "Structure of the Guadaloupe Box Area, Sandoval County, New Mexico," New Mexico Geol. Soc. Twenty-Fifth Field Conf., Ghost Ranch: Central-Northern New Mexico (1974).

14. L. A. Woodward, R. Martinez, H. R. Duchene, O. L. Schumacher, and R. K. Reed, "Precambrian Rocks of the Southern Sierra Nacimiento, New Mexico," New Mexico Geol. Soc. Twenty-Fifth Field Conf., Ghost Ranch: Central-Northern New Mexico (1974).

15. D. B. Clarke and A. C. Eddy, "Systematic Identification of Feldspars in Thin Section," in Geology 301: Igneous Petrology Laboratory Manual, Second Edition, (Dalhousie Univ. Press, Halifax, N.S., Canada, 1973), pp 18-20.

16. L. Van der Plas and A. C. Tobi, "A Chart for Judging the Reliability of Point Counting Results," Am. Journ. Sc. 263, 87-90 (January 1965).

17. A. G. Blair, J. W. Tester, and J. J. Mortensen, "LASL Hot Dry Rock Geothermal Project July 1, 1975 - June 30, 1976," Los Alamos Scientific Laboratory Report LA-6525-PR (1976).

18. N. L. Carter, "Steady State Flow of Rocks," Rev. of Geophys. and Space Phys. v. 14, p. 301-360 (1976).

19. R. A. Heimlich, "Morphology of Zircons from Precambrian Rocks Penetrated by Geothermal Test Hole GT-2," Los Alamos Scientific Laboratory Report LA-6433-MS (July 1976).

20. D. G. Brookins and A. W. Laughlin, "Rubidium-Strontium Geochronologic Study of GT-1 and GT-2 Whole Rocks," EOS, Trans. Amer. Geophys. Un., v. 57, p. 352 (1976).

21. C. W. Naeser and R. B. Forbes, "Variation of Fission Track Ages With Depth in Two Deep Drill Holes," EOS, Trans. Amer. Geophys. Un., v. 57, p. 352 (1976).

22. D. L. Turner and R. B. Forbes, "K-Ar Studies in Two Deep Basement Drill Holes: A New Geologic Estimate of Argon Blocking Temperature for Biotite," EOS, Trans. Amer. Geophys. Un., v. 57, p. 352 (1976).

23. F. G. West and A. W. Laughlin, "Spectral Gamma Logging in Crystalline Basement Rocks," Geology, v. 4, p. 617-618 (1976).

TABLE I

PHANEROZOIC SECTION IN LASL DRILL HOLES

	Drill Hole					
	A[a]	B[a]	C[a]	D[a]	GT-1[b]	GT-2[b]
Surface elevation m	2575.6	2628.9	2651.8	2407.9	2583.2	2648.7
Thickness						
Bandelier Tuff	9.1	115.8	73.2	36.6	18.3	106.7
Tschicoma Formation	-	18.3	-	-	-	-
Paliza Canyon Formation	-	-	-	-	-	15.2
Abiquiu Tuff	38.1	-	103.6	-	30.5	15.2
Abo Formation	102.1	64.0	51.8	115.8	277.4	237.7
Magdalena Group						
Madera Limestone	-	-	-	-	227.1	275.9
Sandia Formation	-	-	-	-	88.4	79.3

[a] Drill Holes A, B, C, D bottomed in Abo Formation.

[b] Drill Holes GT-1, GT-2 bottomed in Precambrian.

TABLE II

A. CORE SUMMARY OF GT-2

Core No.	Depth (m(ft))	Recovery (%)	Lithology
1	633-639 (2078-2098)	25	Clay, limestone fragments
2	685-688 (2248-2258)	<10	Shale, limestone fragments
3	776-786 (2547-2580)	26	Leucocratic monzogranite gneiss
4	739-792 (2590-2600)	70	Leucocratic monzogranite gneiss
5	863-867 (2831-2844)	29	Leucocratic syenogranite gneiss
6	867-871 (2844-2857)	23	Leucocratic monzogranite gneiss
7	960-970 (3151-3182)	23	Biotite-granodiorite gneiss
8	1056-1059 (3464-3476)	16	Leucocratic monzogranite gneiss
9	1127-1129 (3694-3705)	100	Leucocratic monzogranite gneiss, granodiorite gneiss, pegmatite
10	1304-1306 (4278-4285)	100[a]	Leucocratic monzogranite, gneiss, pegmatite
11	1491-1493 (4892-4897)	100[a]	Leucocratic monzogranite gneiss, leucocratic granodiorite gneiss, minor biotite-tonalite gneiss
12	1498-1500 (4915-4921)	100	Leucocratic monzogranite gneiss
13	1595-1597 (5234-5240)	50	Biotite-granodiorite gneiss, tonalite gneiss
14	1672.4-1674.1 (5487-5492.5)	100[a]	Leucocratic monzogranite gneiss, thin folia of magnetite
15	1723-1725 (5654-5660)	100	Hornblende-biotite schist
16	1823-1825 (5980-5986)	100	Hornblende-biotite-plagioclase schist, amphibolite, granite gneiss, biotite-granodiorite gneiss
17	1875-1876 (6150-6156)	67	Leucocratic granite gneiss, granodiorite gneiss
18	1876-1878 (6156-6162)	100	Granodiorite gneiss
19	1934-1935 (6344-6350)	17	Leucocratic monzogranite gneiss
20	1935-1937 (6350-6356)	~0	Chips of granite gneiss and schist
21	2041-2042 (6695-6701)	0	—
22	2165-2165.2 (7102-7103.7)	100[a]	Biotite-tonalite gneiss and monzogranite gneiss
23	2413-2413.6 (7918-7918.6)	100[a]	Leucocratic monzogranite gneiss
24	2614-2617 (8577-8587)	70	Biotite granodiorite, pegmatite
25	2901-2904 (9519-9527)	50	Biotite granodiorite, monzogranite
26	2904-2907 (9527-9537)	50	Biotite granodiorite
27	2928-2929 (9607-9609)	75	Biotite-granodiorite gneiss

B. CORE SUMMARY OF EE-1

1	2095-2099 (6874-6886)	25	Leucocratic monzogranite gneiss
2	3011-3012 (9877-9881)	17[a]	Leucocratic granodiorite

[a]Diamond cores

TABLE III

MODAL ANALYSES[a] OF PRECAMBRIAN ROCKS FROM GT-2

	2580-26	2600-3	2844-2	2857-13a,b	3151-5A	3464-1b,1c	3464-11	3694-1.1	3696-1.1a,b	3696-1.2	3699-2.1	3703-2.1	4279-2	4280	4281-4
K-feldspar	36±2	29±3	41±3	33±3	8±2	33±3	25±3	29±2	29±3	23±3	33±3	15±2	30±3	30±3	31±3
Plagioclase	32±2	34±3	18±2	24±3	45±3	28±3	31±3	32±2	27±3	34±3	28±3	40±3	29±3	32±3	29±3
(% An)	(34)	(23)	(30)	(34)	(22)	(33)	(33)	(29)	(31)	(32)	(30)	(28)	(31)	(31)	(32)
Quartz	25±2	29±3	38±3	39±3	25±3	36±3	38±3	33±2	36±3	38±3	33±3	32±3	33±3	30±3	32±3
Biotite	1	5±1	-	Tr	13±2	<0.5	2±1	<1	6±1	<0.5	<0.5	8±1	3±1	2±1	2±1
Chlorite	3±1	<0.5	<1	<1	Tr	Tr	<0.5	<0.5	<0.5	<1	2±1	Tr	1	1	1
Opaques	1	2	2	1	3±1	<1	1	<0.5	Tr	<1	1	<0.5	<0.5	<0.5	<1
Muscovite	1	<1	<1	<1	2	Tr	2±1	<1	<0.5	1	<1	4±1	3±1	3±1	2±1
Myrmekite	<1	<1	-	2±1	Tr	2±1	<1	4±1	2±1	2±1	<1	Tr	1	<1	<0.5
Calcite	<0.5	Tr	Tr	Tr	2	Tr	<0.5	<0.5	Tr	<1	<1	Tr	<0.5	<0.5	<1
Epidote[b]	<0.5	Tr	Tr	Tr	2	Tr	Tr?	Tr?	Tr	<0.5	Tr	Tr	<0.5	<0.5	<0.5
Apatite	<0.5	<0.5	Tr	Tr?	Tr	-	<0.5	Tr	<0.5	<0.5	<0.5	<1	Tr	Tr	-
Sphene	Tr?	-	-	-	-	Tr	Tr?	-	<0.5	<0.5	-	Tr?	-	-	-
Zircon	Tr?	Tr	-	-	Tr	Tr	Tr	Tr	Tr	Tr?	Tr	Tr	Tr	Tr	-
Amphibole	-	-	-	-	-	-	-	-	-	-	-	-	-	-	-
Others	-	-	Tr	Tr	-	Tr	Tr	Tr	-	-	Tr	Tr	Tr	Tr	Tr
Number of Counts	1637	1277	1406	1181	1016	1076	1175	1542	1270	859	1318	1443	880	992	1121
Rock Type	Leucocratic monzogranite gneiss	Leucocratic monzogranite gneiss	Leucocratic syenogranite gneiss	Leucocratic monzogranite gneiss	Biotite-granodiorite gneiss	Leucocratic monzogranite gneiss	Leucocratic monzogranite gneiss	Leucocratic monzogranite gneiss	Leucocratic monzogranite gneiss	Leucocratic monzogranite gneiss	Leucocratic monzogranite gneiss	Granodiorite gneiss	Leucocratic monzogranite	Leucocratic monzogranite	Leucocratic monzogranite

[a] Tr ≤0.10% .

[b] Epidote group minerals, one or more of varieties pistacite, clinozoisite, and non-ferrian zoisite.

TABLE III (cont'd)

MODAL ANALYSES[a] OF PRECAMBRIAN ROCKS FROM GT-2

	4282-4	4892-1b,1b1-(Felsic),1b2	4893-1a and 4892-1b1-(Mafic)	4893-1b	4895-2a,2b	4896-2a	4917-2a	4919-5	4920-3	5234-5	5234-10	5234-11a,11b	5240-1A	5240-1B
K-feldspar	21±2	15±1	-	28±3	24±2	28±3	31±3	28±3	33±3	12±2	<1	16±2	11±2	37±3
Plagioclase	35±3	43±2	59±2	31±3	30±2	31±3	27±3	31±3	37±3	34±3	53±3	39±2	44±3	31±3
(% An)	(31)	(34)	(29)	(33)	(32)	(34)	(28)	(32)	(28)	(35)	(25)	(34)	(33)	(35)
Quartz	34±3	39±2	22±2	38±3	39±2	36±3	36±3	35±3	25±3	28±3	32±3	34±2	32±3	31±3
Biotite	4±1	2	16±2	<0.5	3±1	2±1	3±1	2±1	2±1	-	10±2	8±1	5±1	-
Chlorite	<1	0.5	1	<1	2±1	1	1	<1	1	16±2	<0.5	<1	3±1	Tr
Opaques	<0.5	Tr	Tr	<1	<1	<1	<0.5	<1	Tr	<0.5	<1	<0.5	<1	<0.5
Muscovite	4±1	Tr	<0.5	<0.5	<0.5	Tr	<0.5	Tr	0.5	2±1	Tr	Tr	Tr	Tr
Myrmekite	<1	Tr	-	<1	<1	<0.5	1	2±1	2±1	-	Tr	Tr	Tr	-
Calcite	0.5	Tr	<0.5	<0.5	<0.5	<0.5	Tr	Tr	<0.5	<1	<0.5	Tr	Tr	Tr
Epidote[b]	<0.5	Tr	1	<0.5	<1	<0.5	<0.5	<0.5	<0.5	7+2	<1	Tr	2±1	<1
Apatite	Tr	Tr	<0.5	Tr	Tr	Tr	Tr	Tr	Tr	Tr	<0.5	Tr	Tr	Tr
Sphene	-	Tr	<0.5	<0.5	-?	Tr	-	0.5	Tr	<1?	Tr?	Tr	Tr	Tr?
Zircon	Tr?	Tr	Tr	-	Tr	Tr	Tr	Tr	Tr	-	Tr	Tr	Tr	-
Amphibole	-	-	<0.5	-	<0.5	Tr	Tr	-	-	-	3±1	2	2±1	-
Other	Tr	Tr	<0.5	Tr	<0.5	Tr	-	Tr	Tr	<0.5	Tr	Tr	Tr	Tr
Number of Counts	1201	3971	2159	1457	2432	1108	1114	918	1053	867	857	1903	1196	1096
Rock Type	Leucocratic monzogranite	Leucocratic granodiorite gneiss	Biotite-tonalite gneiss	Leucocratic monzogranite gneiss	Leucocratic monzogranite gneiss	Leucocratic monzogranite gneiss	Leucocratic monzogranite gneiss	Leucocratic monzogranite gneiss	Leucocratic monzogranite gneiss	Metamorphosed granodiorite gneiss	Biotite-tonalite gneiss	Biotite-granodiorite gneiss	Biotite-granodiorite gneiss	Leucocratic monzogranite gneiss

[a] Tr ≤0.10% .

[b] Epidote group minerals, one or more of varieties pistacite, clinozoisite, and non-ferrian zoisite.

TABLE III (cont'd)

MODAL ANALYSES[a] OF PRECAMBRIAN ROCKS FROM GT-2

	5487-M-1	5492-1d1,1d2	5654-2b	5980-1	5980-2b,2c	5983-3b	5985-5b,5c (Mafic)	5985-5b,5c (Felsic)	6152-3	6153-4c	6155-26	6159-2c1	6160-4	6344-6350-3
K-feldspar	36±3	30±3	-	33±3	<1	1	Tr	11±2	40±3	22±2	9±2	11±2	10±2	29±3
Plagioclase	22±3	22±3	40±3	17±2	44±3	40±3	43±3	26±3	22±3	42±3	46±3	37±3	38±3	23±3
(% An)	(34)	(34)	(36)	(33)	(34)	(38)	(35)	(35)	(32+)	(33)	(37)	(36)	(33)	(33)
Quartz	39±3	42±3	17±2	43±3	22±3	6±1	7±1	47±3	35±3	28±3	35±3	40±3	41±3	44±3
Biotite	<0.5	<0.5	29±3	5±1	12±2	2±1	12±2	9±2	<0.5	5±1	6±1	5±1	7±2	Tr
Chlorite	<0.5	<1	Tr	Tr?	Tr	Tr	Tr	3±1	-	<1	<1	Tr	<1	<0.5
Opaques	0.5	4±1	<1	<0.5	<0.5	1	<0.5	<1	<1	<1	2±1	2±1	2±1	1
Muscovite	<1	0.5	<0.5	Tr	<1	Tr	14±2	3±1	0.5	1	1	<1	Tr	1
Myrmekite	2±1	<1	-	2±1	-	-	-	-	Tr	Tr	Tr	Tr	<1	<1
Calcite	0.5	-	-	-	Tr	<1	9±2	Tr	1	<1	Tr	4±1	1	<1
Epidote[b]	Tr	Tr?	<1	Tr?	3±1	<1	2±1	Tr	Tr	Tr	Tr	Tr	-	Tr
Apatite	-	Tr	1	Tr	Tr	Tr	Tr	Tr	Tr	Tr	Tr	Tr	Tr	Tr
Sphene	Tr?	Tr	<1	Tr?	-	-	-	-	-	Tr	Tr	-	-	≤0.5?
Zircon	Tr	Tr	Tr	Tr	Tr	-	-	Tr	-	Tr	Tr	-	-	Tr
Amphibole	-	-	11±2	-	18±3	47±2	13±2	-	-	-	-	-	-	-
Others	Tr	-	Tr	Tr	Tr	-	-	-	-	-	-	-	-	-
Number of Counts	1040	1046	1120	931	930	1000	1139	889	876	1141	969	1000	1007	1043
Rock Type	Leucocratic monzogranite gneiss	Leucocratic monzogranite gneiss	Hornblende-biotite-plagioclase schist	Granite gneiss	Quartzo-feldspathic biotite-hornblende schist	Amphibolite	Hornblende-mica-plagioclase schist	Quartz-rich biotite-granodiorite gneiss	Leucocratic granite gneiss	Leucocratic granodiorite gneiss	Granodiorite gneiss	Leucocratic granodiorite gneiss	Biotite-granodiorite gneiss	Leucocratic monzogranite gneiss

[a] Tr ≤0.10% .

[b] Epidote group minerals, one or more of varieties pistacite, clinozoisite, and non-ferrian zoisite.

TABLE III (cont'd)

MODAL ANALYSES[a] OF PRECAMBRIAN ROCKS FROM GT-2

	7103-1c,1j1	7103-1g1,1g2	7103-1i	7918-1a	8578-2	9519-1	9521-1	9531-1a	9607-2a,2b	9607-M1	9608-2b2	9608-2b3
K-feldspar	39±3	Tr?	<0.5	30±3	21±3	15±2	29±3	20±2	7±1	9±2	12±1	8±1
Plagioclase	31±3	47±2	50±3	24±3	34±3	38±3	34±3	37±3	41±2	45±3	43±2	51±3
(% An)	(35)	(35)	(25)	(33)	(31+)	(33)	(33)	(36+)	(34)[d]	(34)	(36)	(34)
Quartz	29±3	35±2	23±3	42±3	29±3	25±3	32±3	23±3	35±2	32±3	31±2	26±2
Biotite	Tr	14±2	11±2	<1	11±2	13±2	0.5	13±2	14±2	11±2	10±1	11±1
Chlorite	<0.5	2±1	<0.5	<0.5	<0.5	Tr	<1	<1	Tr	Tr	Tr	Tr
Opaques	<0.5	<1	<0.5	1	1	1	<1	<1	0.5	<1	2±1	1
Muscovite	0.5	Tr	Tr	<1	<0.5	<1	2±1	<0.5	Tr	<0.5	<0.5	<0.5
Myremekite	Tr	Tr	Tr	<0.5	1	<1	Tr?	1	0.5	<1	<1	0.5
Calcite	<0.5	<0.5	-	<0.5	<0.5	Tr	Tr	<1	Tr	Tr	<0.5	<0.5
Epidote[b]	<0.5	<1	3±1	0.5	1	3±1	2±1	1	<1	2±1	1	2±1
Apatite	-	<1	Tr	Tr	<1	<1	-	<1	Tr	Tr	Tr	Tr
Sphene	-	-	-	Tr	2±1	2±1	Tr	2±1	2±1	<0.5	<0.5	<1
Zircon	Tr	Tr	Tr?	Tr	Tr	Tr	-	Tr	Tr	Tr	Tr	-
Amphibole	-	-	13±2	-	-	-	-	<0.5	-	-	-	-
Others	<0.5	Tr	-	Tr	Tr?	Tr	Tr	-	Tr	Tr?	-	-
Number of Counts	1058	1735	953	1138	1000	1021	829	1011	1805	907	1787	1719
Rock Type	Leucocratic monzogranite gneiss	Biotite-tonalite gneiss	Biotite-hornblende-tonalite gneiss	Leucocratic monzogranite gneiss	Biotite granodiorite[c]	Biotite granodiorite	Leucocratic monzogranite	Biotite granodiorite[c]	Biotite-granodiorite gneiss	Biotite-granodiorite gneiss	Biotite-granodiorite gneiss	Biotite-granodiorite gneiss

[a] Tr ≤0.10% .

[b] Epidote group minerals, one or more of varieties pistacite, clinozoisite, and non-ferrian zoisite.

[c] Determined to be same unit as 9519-1 from chemical, petrographic, and geophysical evidence, although 8578-2 and 9531-1a modes plot in the IUGS monzogranite field.

[d] One relatively large grain with prominent close-spaced fractures perpendicular to the twinning yields An_{45} by optical methods awaiting confirmation by microprobe analysis.

TABLE IV

AVERAGE MODAL ANALYSES[a] (%) OF THE MAJOR PRECAMBRIAN ROCK UNITS IN GT-2

	Major Banded Gneiss			Monzogranitic Dike (Granitoid)	Biotite Granodioritic Units		Mafic Rocks	
	24 Granitic	11 Granodioritic	4 Tonalitic	4 Granites	3 Biotite Granodiorites (Granitoid)[b]	4 Biotite--Granodiorite Gneisses	3 Schists	1 Amphibolite
K-feldspar (Microcline)	31	13	<0.5	28	19	9	<0.5	1
Plagioclase feldspar	28	39	53	31	36	45	42	40
(An content)	(32)	(33)	(29)	(31)	(33)	(35)	(35)	(38)
Quartz	36	35	28	32	26	31	15	6
Biotite	1	1	13	3	12	12	18	2
Chlorite	1	7	1	<1	<0.5	Tr	Tr	Tr
(Ti-) magnetite	<1	<0.5	<0.5	<0.5	1	1	-	-
Leucoxene	<0.5	<1	Tr	Tr	-	Tr	<0.5	<1
Hematite (Opaques)	Tr	Tr	Tr	Tr	-	Tr	-	Tr
Pyrite	Tr	<0.5	Tr	-	<0.5	Tr?	<0.5	<0.5
Opaques	1	1	0.5	1	1	1	0.5	1
Muscovite	<1	2	<0.5	3	<0.5	<0.5	5	Tr
Myrmekite	1	<0.5	Tr	<1	<1	<1	-	-
Calcite	<0.5	1	<0.5	<1	<0.5	Tr	3	<1
Epidote	<0.5	1	1	<0.5	2	1	2	<1
Apatite	<1	<1	<0.5	Tr	<1	Tr	<0.5	Tr
Sphene	<0.5	<1	Tr	-	2	1	<0.5	-
Zircon	Tr	Tr	Tr	Tr	Tr	Tr	Tr	-
Amphibole	Tr	<1	4	-	Tr	-	14	47
Other	Tr	Tr	Tr	Tr	Tr	Tr	Tr	-

[a] Tr $\leq$0.10% .

[b] Exclusive of felsic segregation, of monzogranite composition.

TABLE V

CHEMICAL ANALYSES OF PRECAMBRIAN ROCKS FROM GT-2 AND EE-1[a]

Sample No.	2580-26	2600-3	2844-2	3151-5a	3464-11	3464-16c	3694-1.1
Oxides							
SiO_2	73.86	72.85	75.78	65.05	75.87	77.43	75.43
TiO_2	0.35	0.30	0.08	0.56	0.30	0.11	0.12
Al_2O_3	12.35	13.15	12.35	16.00	11.70	11.98	12.95
Fe_2O_3	1.58	1.24	0.53	1.13	1.23	0.34	0.72
FeO	2.00	1.93	0.90	2.89	1.03	0.38	1.21
MgO	0.67	0.68	0.07	1.46	0.20	0.03	0.18
CaO	1.72	1.32	0.45	3.15	1.00	0.69	0.88
MnO	0.074	0.050	0.015	0.079	0.046	0.015	0.036
SrO	0.011	0.011	0.004	0.043	0.012	0.004	0.009
Na_2O	3.71	3.25	3.0	4.50	3.27	3.43	3.25
K_2O	2.16	3.72	5.50	2.89	3.81	4.68	4.15
$H_2O^{(-)}$	0.07	0.09	0.08	0.12	0.02	0.07	0.05
$H_2O^{(+)}$	0.48	0.54	0.30	1.22	0.89	0.54	0.58
CO_2	0.33	0.14	0.07	0.69	<0.01	<0.01	0.00
P_2O_5	0.10	0.10	0.02	0.18	0.05	<0.01	0.04
Total	99.46	99.37	99.15	99.96	99.43	99.79	99.61
Barth Catanorm							
ap	0.22	0.22	0.04	0.38	0.11	0.00	0.09
il	0.50	0.43	0.11	0.80	0.43	0.16	0.17
cc	0.00	0.00	0.00	0.00	0.00	0.00	0.00
or	13.19	22.66	33.41	17.43	23.30	28.26	25.16
ab	34.43	30.09	27.70	41.24	30.39	31.48	29.95
mt	1.71	1.34	0.57	1.21	1.33	0.36	0.77
hm	0.00	0.00	0.00	0.00	0.00	0.00	0.00
an	8.14	6.08	2.16	14.75	4.80	3.50	4.21
C	1.15	1.82	0.78	0.19	0.56	0.02	1.80
Q	37.08	33.60	34.05	16.79	38.10	35.90	36.04
hy	3.58	3.78	1.17	7.21	0.98	0.32	1.81
Di	0.00	0.00	0.00	0.00	0.00	0.00	0.00

[a]All analyses are from GT-2 unless designated EE-1.

TABLE V (Cont'd.)

CHEMICAL ANALYSES OF PRECAMBRIAN ROCKS FROM GT-2 AND EE-1[a]

Sample No.	3699-2.1	3703-2.1	4279-2	4280	4282-M-4	4896-2	4917-2
Oxides							
SiO_2	74.42	73.30	72.49	72.15	71.60	73.45	74.27
TiO_2	0.13	0.13	0.17	0.18	0.22	0.28	0.22
Al_2O_3	12.80	13.90	13.90	14.42	14.28	12.80	12.50
Fe_2O_3	0.57	0.64	0.60	0.71	0.70	1.18	1.08
FeO	1.08	1.97	1.20	1.38	1.53	1.65	1.40
MgO	0.24	0.66	0.40	0.46	0.48	0.23	0.18
CaO	0.77	1.80	0.99	1.10	1.28	1.09	1.03
MnO	0.040	0.087	0.047	0.050	0.052	0.065	0.052
SrO	0.011	0.017	0.016	0.016	0.018	0.015	0.014
Na_2O	3.11	3.75	3.15	3.35	3.50	3.20	3.40
K_2O	5.05	2.05	5.30	4.68	4.21	4.75	4.33
$H_2O^{(-)}$	0.02	0.09	0.13	0.11	0.18	0.06	0.24
$H_2O^{(+)}$	0.59	0.98	0.96	1.05	1.17	0.64	0.80
CO_2	0.18	0.14	0.03	0.04	0.23	0.00	0.17
P_2O_5	0.05	0.09	0.04	0.05	0.05	0.04	0.025
Total	99.06	99.79	99.42	99.75	99.50	99.45	99.71
Barth Catanorm							
ap	0.11	0.19	0.09	0.11	0.11	0.09	0.06
il	0.19	0.44	0.24	0.26	0.32	0.40	0.40
cc	0.00	0.00	0.00	0.00	0.00	0.00	0.00
or	30.78	12.45	32.18	28.33	25.64	28.89	26.37
ab	28.81	34.62	29.07	30.82	32.40	29.58	31.47
mt	0.61	0.69	0.64	0.76	0.75	1.27	1.16
hm	0.00	0.00	0.00	0.00	0.00	0.00	0.00
an	3.60	8.58	4.78	5.26	6.21	5.30	5.07
C	1.06	2.76	1.43	2.20	1.98	0.57	0.47
Q	32.97	36.00	29.18	29.47	29.52	31.75	33.35
hy	1.88	4.25	2.45	2.81	3.07	2.15	1.65
Di	0.00	0.00	0.00	0.00	0.00	0.00	0.00

[a]All analyses are from GT-2 unless designated EE-1.

TABLE V (Cont'd.)

CHEMICAL ANALYSES OF PRECAMBRIAN ROCKS FROM GT-2 AND EE-1[a]

Sample No.	4919-5	4920-3G	4920-3Peg	5234-10	5234-11	5487-M1	5492-M-1
Oxides							
SiO_2	73.52	71.04	73.20	68.88	67.76	75.67	29.35
TiO_2	0.31	0.14	0.05	0.54	0.62	0.12	3.20
Al_2O_3	12.55	15.58	14.50	14.74	13.78	11.90	1.53
Fe_2O_3	1.26	0.20	0.19	1.49	1.73	1.12	31.97
FeO	1.79	0.76	0.65	2.64	3.71	0.79	23.65
MgO	0.24	0.12	0.08	1.05	1.34	0.08	0.51
CaO	1.04	1.05	1.20	2.91	2.92	0.46	0.50
MnO	0.068	0.022	0.015	0.097	0.161	0.029	0.44
SrO	0.014	0.016	0.015	0.014	0.014	0.004	0.006
Na_2O	3.25	4.18	4.70	4.99	4.35	3.00	0.035
K_2O	4.48	5.83	4.24	1.46	1.94	5.43	0.10
$H_2O^{(-)}$	0.12	0.08	0.18	0.22	0.18	0.19	0.30
$H_2O^{(+)}$	0.86	0.58	0.61	0.75	1.00	0.53	-
CO_2	0.04	0.00	0.05	0.28	0.33	0.08	-
P_2O_5	0.03	0.028	0.01	0.16	0.157	0.005	0.180
Total	99.57	99.63	99.69	100.22	99.99	99.41	98.98
Barth Catanorm							
ap	0.06	0.06	0.02	0.42	0.34	0.06	0.57
il	0.32	0.20	0.07	0.76	0.89	0.17	6.06
cc	0.00	0.00	0.00	0.00	0.00	0.00	0.00
or	27.35	34.70	25.29	8.75	11.77	33.08	0.80
ab	30.15	37.81	42.60	45.46	40.11	27.78	0.49
mt	1.36	0.21	0.20	1.58	1.86	1.21	45.42
hm	0.00	0.00	0.00	0.00	0.00	0.00	0.00
an	5.13	5.05	5.95	13.48	12.68	2.15	1.60
C	0.60	0.61	0.02	0.09	0.00	0.36	1.37
Q	32.58	20.17	24.81	24.17	24.14	34.62	27.36
hy	2.44	1.18	1.04	5.27	7.32	0.56	16.34
Di	0.00	0.00	0.00	0.00	0.90	0.00	0.00

[a]All analyses are from GT-2 unless designated EE-1.

TABLE V (Cont'd.)

CHEMICAL ANALYSES OF PRECAMBRIAN ROCKS FROM GT-2 AND EE-1[a]

Sample No.	5654-1	5654-2b,c	6160-4	6344/ 6350-4,6	7103-1A[2]	7103-1E[3]	7103-1H[4]
Oxides							
SiO_2	55.08	55.11	68.91	75.93	75.43	71.01	65.14
TiO_2	1.40	1.47	0.44	0.06	0.06	0.46	0.49
Al_2O_3	15.62	15.45	14.00	12.30	12.80	13.29	15.43
Fe_2O_3	1.92	1.82	1.50	0.68	0.53	1.34	1.69
FeO	7.27	7.00	2.43	0.87	0.63	2.93	3.92
MgO	4.54	4.80	0.96	0.08	0.14	1.10	2.02
CaO	5.22	5.05	1.70	0.43	0.64	2.26	3.55
MnO	0.146	0.136	0.067	0.017	0.012	0.068	0.128
SrO	0.022	0.023	0.022	0.004	0.014	0.019	0.017
Na_2O	3.00	2.73	3.86	3.22	2.44	3.83	4.21
K_2O	3.01	3.61	3.40	5.04	6.50	2.09	1.83
$H_2O^{(-)}$	0.10	0.115	0.28	0.09	0.10	0.03	0.16
$H_2O^{(+)}$	1.26	1.29	1.41	0.72	0.58	1.01	1.10
CO_2	0.47	0.49	0.58	<0.05	<0.05	<0.05	0.15
P_2O_5	0.505	0.52	0.11	0.01	<0.01	0.12	0.14
Total	99.56	99.61	99.67	99.45	99.88	99.56	99.98
Barth Catanorm							
ap	1.08	1.13	3.43	0.02	0.02	0.26	0.30
il	2.01	2.13	0.63	0.09	0.09	0.66	0.70
cc	0.00	0.00	0.00	0.00	0.00	0.00	0.00
or	18.35	22.14	20.58	30.62	39.33	12.72	11.03
ab	27.80	25.45	35.51	29.73	22.44	35.43	38.58
mt	2.07	1.98	1.61	0.73	0.57	1.44	1.80
hm	0.00	0.00	0.00	0.00	0.00	0.00	0.00
an	20.92	19.27	0.00	2.13	3.19	10.75	17.05
C	0.00	0.28	4.44	0.89	0.68	1.02	0.45
Q	5.40	5.83	29.24	34.72	32.74	31.42	19.89
hy	20.43	21.80	4.99	1.07	0.95	6.30	10.20
Di	1.95	0.00	0.00	0.00	0.00	0.00	0.00

[a] All analyses are from GT-2 unless designated EE-1.

[b] This analysis corresponds to thin section no. 7103-1c.

[c] This analysis corresponds to thin section no. 7103-1g.

[d] This analysis corresponds to thin section no. 7103-1i.

TABLE V (Cont'd.)

CHEMICAL ANALYSES OF PRECAMBRIAN ROCKS FROM GT-2 AND EE-1[a]

Sample No.	9607-M7	9607-2b	EE-1/6875-2	EE-1/9877-2b
Oxides				
SiO_2	67.92	69.29	76.53	75.09
TiO_2	0.80	0.80	0.10	0.08
Al_2O_3	14.47	13.60	12.76	13.16
Fe_2O_3	1.83	1.57	0.62	0.42
FeO	2.58	2.59	0.68	0.48
MgO	1.42	1.40	0.05	0.21
CaO	3.38	3.02	0.44	1.26
MnO	0.088	0.082	0.04	0.03
SrO	0.032	0.030	0.00	0.020
Na_2O	3.38	3.32	3.30	3.29
K_2O	2.62	2.70	5.17	4.87
$H_2O^{(-)}$	0.00	0.00	0.00	0.02
$H_2O^{(+)}$	0.65	0.73	0.40	0.56
CO_2	0.23	0.14	0.04	0.06
P_2O_5	0.18	0.18	0.01	0.02
Total	99.58	99.45	100.14	99.57
Barth Catanorm				
ap	0.39	0.39	0.02	0.04
il	1.15	1.15	0.14	0.11
cc	0.00	0.00	0.00	0.00
or	15.92	16.45	31.04	29.42
ab	31.22	30.74	30.11	30.02
mt	1.97	1.69	0.66	0.45
hm	0.00	0.00	0.00	0.00
an	16.04	14.24	2.15	5.93
C	0.40	0.18	1.06	0.39
Q	27.09	29.18	34.13	32.47
hy	5.83	5.98	0.69	0.99
Di	0.00	0.00	0.00	0.00

[a]All analyses are from GT-2 unless designated EE-1.

TABLE V (Cont'd.)

CHEMICAL ANALYSES OF PRECAMBRIAN ROCKS FROM GT-2 AND EE-1[a]

Sample No.	7918-1b	8583-1A	8583-1B	9519-1	9520-3	9521-M1	9522-1	9529-2
Oxides								
SiO_2	77.16	64.63	65.20	63.20	63.96	75.13	66.31	62.32
TiO_2	0.49	0.79	0.80	1.00	1.02	0.03	0.86	1.24
Al_2O_3	10.20	15.20	14.75	14.49	13.90	12.95	14.01	14.50
Fe_2O_3	2.41	2.33	2.60	3.23	3.49	0.53	2.28	3.83
FeO	1.88	2.87	2.88	3.03	2.84	0.59	2.44	3.46
MgO	0.22	1.31	1.28	1.56	1.38	0.12	1.30	1.53
CaO	1.18	2.63	2.99	3.28	3.28	0.80	2.45	4.03
MnO	0.070	0.081	0.080	0.103	0.092	0.034	0.08	0.104
SrO	0.019	0.042	0.047	0.046	0.043	0.005	0.040	0.046
Na_2O	2.74	3.08	3.15	3.75	3.22	4.02	3.44	3.28
K_2O	2.92	5.15	4.31	3.90	3.94	4.92	4.50	3.60
$H_2O^{(-)}$	0.18	0.03	0.06	0.12	0.08	0.09	0.07	0.05
$H_2O^{(+)}$	0.58	0.79	0.87	1.00	1.27	0.61	0.95	0.99
CO_2	<0.05	0.15	0.15	0.30	0.40	<0.05	0.38	0.15
P_2O_5	0.04	0.57	0.58	0.55	0.59	<0.01	0.44	0.68
Total	100.09	99.65	99.75	99.55	99.50	99.83	99.55	99.81
Barth Catanorm								
ap	0.09	1.22	1.25	1.17	1.29	0.02	0.95	1.47
il	0.71	1.13	1.15	1.44	1.48	0.04	1.24	1.79
cc	0.00	0.00	0.00	0.00	0.00	0.00	0.00	0.00
or	17.97	31.24	26.23	23.87	24.28	29.48	27.56	22.01
ab	25.63	28.40	29.13	34.89	30.15	36.61	32.02	30.48
mt	2.62	2.50	2.80	3.50	3.81	0.56	2.47	4.14
hm	0.00	0.00	0.00	0.00	0.00	0.00	0.00	0.00
an	5.83	9.57	11.38	11.24	12.35	2.80	7.24	14.71
C	0.55	1.28	0.96	0.14	0.00	0.00	1.04	0.00
Q	45.29	19.04	21.76	18.04	21.72	29.12	22.58	19.31
hy	1.32	5.61	5.35	5.71	4.45	0.43	4.88	4.98
Di	0.00	0.00	0.00	0.00	0.48	0.93	0.00	1.11

[a]All analyses are from GT-2 unless designated EE-1.

TABLE VI

CHEMICAL COMPOSITIONS OF TYPICAL PRECAMBRIAN ROCKS FROM GT-2

	(1)	(2)	(3)	(4)	(5)
SiO_2	64.27	72.08	55.10	65.05	77.43
TiO_2	0.95	0.19	1.44	0.56	0.11
Al_2O_3	14.48	14.20	15.54	16.00	11.98
Fe_2O_3	2.96	0.67	1.87	1.13	0.34
FeO	2.92	1.37	7.14	2.89	0.38
MgO	1.39	0.45	4.67	1.46	0.03
CaO	3.11	1.12	5.14	3.15	0.69
MnO	0.091	0.050	0.140	0.079	0.015
SrO	0.044	0.017	0.023	0.043	0.004
Na_2O	3.32	3.33	2.87	4.50	3.43
K_2O	4.23	4.73	3.31	2.89	4.68
$H_2O^{(-)}$	0.07	0.14	0.11	0.12	0.07
$H_2O^{(+)}$	0.98	1.06	1.28	1.22	0.54
CO_2	0.26	0.10	0.48	0.69	<0.01
P_2O_5	0.57	0.05	0.51	0.18	<0.01

(1) Biotite granodiorite (average of 6 samples).

(2) Leucocratic monzogranite dike (average of 3 samples).

(3) Ferrohastingsite - biotite schist (average of 2 samples).

(4) Biotite granodioritic gneiss. [depth 960 m (3151 ft)].

(5) Leucocratic monzogranitic gneiss [depth 1056 m (3464 ft)].

TABLE VII

COMPARISON OF CHEMICALLY SIMILAR ROCK TYPES

	Av. Schist (GT-2)	Av. Amphibolite[a]	Av. Diorite[b]	Av. Andesite[c]
SiO_2	55.10	50.3	56.77	54.20
TiO_2	1.44	1.6	0.84	1.31
Al_2O_3	15.54	15.7	16.67	17.17
Fe_2O_3	1.87	3.6	3.16	3.48
FeO	7.14	7.8	4.40	5.49
MgO	4.67	7.0	4.17	4.36
CaO	5.14	9.5	6.74	7.92
MnO	0.14	0.2	0.13	0.15
SrO	0.023	-	-	-
Na_2O	2.87	2.9	3.39	3.67
K_2O	3.31	1.1	2.12	1.11
$H_2O^{(-)}$	0.11	-	1.36	0.86
$H_2O^{(+)}$	1.28	-		
CO_2	0.48	-	-	-
P_2O_5	0.51	0.3	0.25	0.28

[a] Poldervaart (1955).

[b] Clarke (1966).

[c] Nockolds (1954).

☆ U.S. GOVERNMENT PRINTING OFFICE: 1977—777-018/115